

Photo-Oxidative Desulfurization of Liquid Fuel by BiVO₄/MXene Nanocomposite



This dissertation is submitted to the department of chemistry,
Quaid-I-Azam University, Islamabad, in partial fulfilment of the
requirements for the degree of

Master of Philosophy

In Inorganic/Analytical Chemistry

By

Saba Gul

Department of Chemistry,

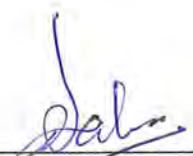
Quaid-i-Azam University Islamabad, Pakistan

2023

DECLARATION


This is to certify that this dissertation entitled **“Photo-Oxidative Desulfurization of Liquid Fuel by BiVO₄/Mxene Nanocomposite”** submitted by *Ms. Saba Gul*, is accepted in its present form by the Department of Chemistry, Quaid-i-Azam University, Islamabad, as satisfying the dissertation requirements for the degree of *Master of Philosophy in Analytical/Inorganic Chemistry*

External Examiner:



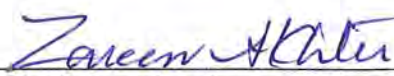
Dr. Saleem A. Bokhari
Associate Professor
Department of Biosciences, Park Road,
Chak Shahzad, COMSATS University,
Islamabad.

Supervisor:




Prof. Dr. Amir Waseem
Department of Chemistry
Quaid-i-Azam University
Islamabad

Head of Section:



Prof. Dr. Mrs. Zareen Akhter
Department of Chemistry
Quaid-i-Azam University
Islamabad

Chairman:



Prof. Dr. Aamer Saeed Bhatti
Department of Chemistry
Quaid-i-Azam University
Islamabad

بِسْمِ اللَّهِ الرَّحْمَنِ الرَّحِيمِ

Dedication

This thesis is dedicated to my affectionate parents whose love, encouragement and prayers make me able to get such success and honour, along with all hardworking and respected teachers.

Author Declaration

I hereby declare that I have done all of this work myself and have not used any sources or tools other than those specified. Further I confirm that this work has not been submitted for any other degree.

SABA QUL

Acknowledgements

Praise and gratitude to **Almighty Allah**, the omnipotent, the omniscient Who showered upon me His blessing throughout of my life. All respect for His Last **Prophet Hazrat Muhammad (P.B.U.H)**, who gave my conscience the essence of belief in Allah.

Foremost, I would like to thank my supervisor, **Prof. Dr. Muhammad Amir Waseem** for his wholehearted interest and dedicated supervision. His inspiring guidance, valuable suggestions and friendly behaviour make me possible to accomplish this tough task. In addition, I express my sincere gratitude to **Prof. Dr. Zareen Akhtar** Head of the Inorganic/Analytical section, and **Prof. Dr. Aamer Saeed Bhatti**, Chairman Department of Chemistry, for providing the necessary facilities to undertake my research work.

I would like to thank my colleague, and Lab Fellows **Ms. Madeeha Rani**, **Ms. Komal**, **Ms. Sadaf Khoso**, **Ms. Aneeqa**, **Ms. Shomaila Noureen**, **Ms. Javeria Sultana**, **Ms. Aira Amin** and **Mr. Muhammad Naeem Khan** for their support throughout my research work.

I would like to extend my sincere gratitude to my dearest friend **Khunsa Ejaz Abbasi** who provided me happiness and distraction, to reset my mind outside of my academic activities.

SABA QUL

Table of Contents

List of Figures	i
List of Tables	iii
List of Abbreviations	iv
Abstract	v
Chapter-1.....	1
1 Introduction.....	1
1.1 Sulfur Compounds in Automobile Fuels.....	2
1.1.1 Gasoline	2
1.1.2 Jet fuel.....	2
1.1.3 Diesel fuel	2
1.2 Sulfur Compounds Composition in Fossil Fuel	3
1.3 The Main Sulfur Compounds Present in Fuel Oil.....	3
1.4 Impact of Sulfur Compounds on Environment	3
1.5 Modern Desulfurization Methods	4
1.5.1 Hydrodesulfurization (HDS).....	5
1.5.2 Non-Hydrodesulfurization Procedures	5
Photo-Oxidative Desulfurization (PODS)	8
1.5.3 Catalytic Systems.....	8
1.5.4 Oxidizing agents used in PODS.....	9
1.5.5 Extraction in PODS.....	10
1.5.6 PODS Methods	10
1.5.7 HDS and ODS Processes	11
1.5.8 Importance of Desulfurization of Fuels	13

1.5.9	Future Challenges to PODS	14
1.5.10	Improvements for PODS.....	14
1.5.11	Advantages of PODS	15
1.5.12	Basic Principle of PODS.....	15
1.6	MXenes as a Co-catalyst.....	18
1.6.1	Struture of MXenes.....	18
1.7	BiVO ₄ as a Photocatalyst	19
1.7.1	Drawbacks of BiVO ₄	20
1.8	Methods to Improve Photocatalytic Efficiency.....	21
1.9	Synthetic Methods for Photocatalyst.....	21
1.9.1	Co-precipitation method	21
1.9.2	Sol-gel method.....	22
1.9.3	Hydrothermal Method.....	22
1.10	Aim and Objectives of Research.....	23
1.11	Plan of research	23
Chapter-2	24
2	Experimental.....	24
2.1	Materials.....	24
2.1.1	Materials for synthesis of MXene.....	24
2.1.2	Materials for the Synthesis of Bismuth Vanadate.....	24
2.2	Synthesis.....	24
2.2.1	Synthesis of MXene	24
2.2.2	Synthesis of Bismuth Vanadate	25
2.2.3	Synthesis of BiVO ₄ / MXene composite	26

2.3	Photo-Oxidative Desulfurization (PODS) of liquid fuel.....	27
2.4	Photocatalytic Studies	27
2.5	Procedure for Tauc Plot Calculations.....	28
2.6	Molar Absorbance Coefficient (ϵ).....	28
Chapter-3.....		30
3	Results and discussions.....	30
3.1	Characterization	30
3.1.1	X-Ray diffraction (XRD).....	30
3.1.2	Scanning electron microscopy (SEM)	32
3.1.3	Energy dispersive X-ray spectroscopy (EDX).....	33
3.2	Optical Study and Band Gap Estimation.....	35
3.3	PODS studies.....	37
3.3.1	Selection of Photocatalyst.....	37
3.3.2	Effect of time.	38
3.3.3	Effect of catalyst dose.....	38
3.3.4	Effect of temperature.	40
3.3.5	Effect of hydrogen peroxide (H_2O_2).	41
3.4	The kinetic studies for photo-oxidative desulfurization (DBT).	42
3.5	Possible Mechanism for the PODS of Liquid Fuel.	43
3.6	Comparative study.....	43
4	Conclusions.....	45
References.....		46

List of Figures

Figure 1.1 Sulfur containing compounds in fossil fuels.	3
Figure 1.2 Non-hydrodesulfurization techniques.	6
Figure 1.3 Simplified overview photo-oxidative desulfurization process.	8
Figure 1.4 Schematic diagram of photo-oxidative desulfurization of liquid fuels.	15
Figure 1.5 The photogeneration process of electron-hole pairs.	17
Figure 1.6 Structure of MAX phase and MXene.	19
Figure 1.7 Properties/features of BiVO ₄ nanoparticles.	20
Figure 1.8 Teflon lined autoclave.	23
Figure 2.1 Synthesis scheme for MXene.	25
Figure 2.2 Synthesis scheme for bismuth vanadate.	26
Figure 2.3 Synthesis scheme for BiVO ₄ /MXene composite.	26
Figure 2.4 Calibration curve for DBT (λ max 284 nm).	29
Figure 3.1 XRD patterns of BiVO ₄ , MXene and BiVO ₄ /MXene composite.	31
Figure 3.2 SEM images of BiVO ₄ at different resolutions.	32
Figure 3.3 SEM images of MXene at different resolutions.	33
Figure 3.4 SEM images of BiVO ₄ /MXene composite at different resolutions.	33
Figure 3.5 EDX analysis of MXene.	34
Figure 3.6 EDX analysis of BiVO ₄	34
Figure 3.7 EDX analysis of BiVO ₄ /MXene composite.	35
Figure 3.8 Tauc plot of BiVO ₄	36
Figure 3.9 Tauc plot of BiVO ₄ /MXene.	36
Figure 3.10 UV-Visible spectra of prepared catalysts for DBT degradation.	37
Figure 3.11 Effect of time on PODS process.	38

Figure 3.12 Effect of catalyst dose on PODS process	39
Figure 3.13 Effect of temperature on PODS process.....	40
Figure 3.14 Effect of Hydrogen peroxide (H ₂ O ₂) on PODS process.....	41
Figure 3.15 Kinetics of PODS process	42

List of Tables

Table 3.1	Calculated crystallite size of synthesized photocatalysts	31
Table 3.2	Comparison of desulfurization of liquid fuel by the PODS from the literature	44

List of Abbreviations

ADS	Adsorption Desulfurization
BDS	Bio-Desulfurization
BT	Benzothiophene
DBT	Dibenzothiophene
EDS	Extraction Desulfurization
H ₂ S	Hydrogen Sulphide
HDS	Hydro-Desulfurization
non-HDS	Non-Hydrodesulfurization
ODS	Oxidative Desulfurization
PODS	Photo-Oxidative Desulphurization
P-XRD	Powder X-ray diffraction
T	Thiophene
Ti ₃ C ₂	Titanium Carbide
USEPA	United State Environmental Protection Agency

Some of catalysts have found their utility in improving the oil quality by eliminating sulfur, such catalysts have gained the remarkable consideration in photo-oxidative desulfurization operation. In today's world, the environmental pollution has become a crucial subject along with the advancement in modern technology and industrialization. In this work, MXene was used as co-catalyst with bismuth vanadate catalyst for photo-oxidative desulfurization process. The catalyst was prepared through one pot hydrothermal method and they were distributed on support surface in a homogeneous manner. Their composition, shape and properties were verified through various characterization techniques like energy dispersive x-ray spectroscopy, x-ray diffraction technique and scanning electron microscopy. Optimization of multiple factors like the oxidizing reagent amount, quantity of catalyst used, and the temperature of reaction was done as they influence greatly on the efficacy of catalyst. A study of the kinetics of the photo-oxidative desulfurization reaction showed that it is a pseudo-first order. The outcomes figured out that by using support, the efficacy of catalyst had been increased by more than 95% and green fuel is obtained.

1 Introduction

The biggest energy resource of world is crude oil, and its need is constantly increasing day by day. It is mainly composed of heteroatomic compounds, hydrocarbons that have straight chains and aromatic compounds.¹ Due to the increase in demand of oil throughout the world, oil resources are continuously depleting and dependence on heavy oils that contains heteroatoms is growing worldwide. So, different research institutes are putting their efforts to transform the heavier oils into lighter form to meet the energy demand that is resulting in increase of sulfur amount into these transformed energy fuels. By using basic processes like chemical treatments and distillation, various petrochemical refineries are successfully converting these heavy oils into profitable amounts like diesel, fuel, aviation fuel and gasoline.² Because of the environmental protection agency rules upgraded methods are being utilized to upgrade the ancient oil refineries.

Burning of fuel in vehicles produce deadly gases, which are controlled by various environment protection organizations in developed countries. To meet the world environmental regulations it is necessary to decrease the content of sulfur in transportation.³ In the modern era desulfurization of fuel oil has become a necessity as sulphur-containing compounds are hazardous for health of human beings as well as other living species.^{4,5}

Sulfur oxides and other hazardous gases are produced during the burning of sulfur-containing compounds such as dibenzothiophenes (DBT), mercaptans, thiophenes (T) and benzothiophenes (BT) which damage the ecosystem and pollute the atmosphere and contaminate the soil as well due to acid rain. The production of fuel that is sulphur free is necessary to satisfy the demands of United State Environmental Protection Agency (USEPA). The amount of sulfur allowed in fuel has been restricted by the USEPA from 10 ppm to 15 ppm.^{6,7}

1.1 Sulfur Compounds in Automobile Fuels

Hydrocarbons such as diesel, petrol and jet fuel are all combined to form petroleum. These fuels are extracted through fractional distillation in accordance with their boiling point range. In thicker distillates, aromatic sulfur species that are heterocyclic are present in greater concentrations while disulfides, mercaptans and sulfides are present in more quantity in the less dense distillates. Different alkylated derivatives and benzothiophene are included in the central distillates, however, the DBT derivatives majorly pollute the diesel streams.⁸

1.1.1 Gasoline

Gasoline is the most desired fuel that is used in automobiles. Its range of boiling is 25°C to 225°C and it is a less dense fraction of raw oil.⁹ Sulfur containing compounds such as thiophenes are present in significant amount.

1.1.2 Jet fuel

The boiling point of kerosene fluctuates in between 130°C to 300°C and it is used majorly as a fuel in jets. Jet fuels are usually comprised of aromatic hydrocarbons along with the substitution of benzothiophenes. Due to the greater stability of sulfur compounds, their degradation is quite difficult.

1.1.3 Diesel fuel

Another most popular fuel that is used for transportation is diesel and it finds its major usage in heavy automobiles such as buses and trucks. Its range of boiling point vary in between 160-380°C. Aliphatic hydrocarbons such as alkanes and cycloalkanes along with the small portion of aromatic hydrocarbons.¹⁰ In the spectra of diesel DBT and BT derivatives have major contribution. The number of carbon atoms in diesel vary from 10 to 15 so, molecular formula is $C_{10}H_{22}$ – $C_{15}H_{32}$.

1.2 Sulfur Compounds Composition in Fossil Fuel

Inactive and active sulfides are two major classifications of sulfides. Active sulfides include the mercaptan, sulfur and hydrogen sulfide while dibenzothiophenes, disulfides and benzothiophenes have been categorized as inactive sulfides. Disulfides, thiols and sulfides have simplest structures that make their desulfurization easy. But aromatic compounds that usually have steric structural hinderance such as benzothiophene, thiophene and dibenzithiophene derivatives are complicated to remove. Hence, the main goal in desulfurization is to eliminate the thiophene derivatives.¹¹

1.3 The Main Sulfur Compounds Present in Fuel Oil

Sulfur compounds present in the fuel include hydrogen sulfide gas which is present in methane reservoirs, sulfides and mercaptans which are found in petrol and pyrites like FeS_2 exist in coal as shown in Figure 1.1.

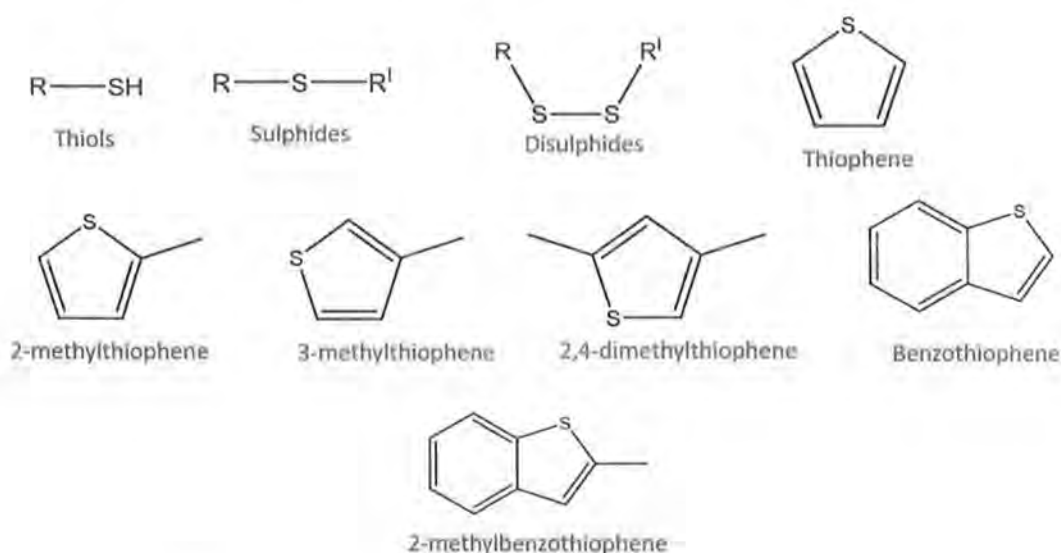


Figure 1.1 Sulfur containing compounds in fossil fuels.

1.4 Impact of Sulfur Compounds on Environment

In these days, the most popular fuels are gasoline and diesel that are used in automobiles. They are obtained from raw oil through fractional distillation process.

Both contain hydrocarbons mixture that's why their chemical and physical properties are closely related.

The economy of any country across the world highly depends upon the energy production by fossil fuel. There are large quantities of sulfur present in fuel which are responsible for release of sulfur oxides in the atmosphere that causes acid rain that's why desulfurization has grabbed more attention.¹²

Removal of sulfur content is necessary from fuel to develop the environmental friendly fuel oil and meet the standard requirements of sulfur in fuel i.e.; 10-15 ppm, according to USEPA.¹³ Purging out of sulfur to refine oil is necessary as the burning of that fuel release harmful gases in the atmosphere that have adverse effects on human health and contaminate the air as well.⁴ So, it is a major aim of material science to develop a cost effective nanomaterial that has the ability to degrade the organic impurities with high efficacy.

Oxides of sulfur are released in the atmosphere due to fuel burning in vehicles which pollute the air and may contaminate with water vapours and cause acid rain, global warming and anxious effects on all living beings such as plants and animals. Acid rain is harmful for buildings, plants, soil and different ecologies. Sulfur from industries may also contaminate the water in lakes, streams and rivers which has detrimental effects on aquatic plants and fishes. The tiny particles of sulfur compounds that remain suspended in air causes smog which is responsible for throat infection, eye irritation and lungs issues. The sulfides such as H_2S that is produced due to fuel burning in engine may cease the appliance as well.

1.5 Modern Desulfurization Methods

There are several available techniques that have been used for sulfur elimination from fuel oil. Among these techniques, extractive desulfurization (EDS), hydrodesulfurization (HDS), photo-oxidative desulfurization (PODS), biological desulfurization (BDS), adsorptive desulfurization (ADS) and Oxidative desulfurization (ODS) are most common. HDS is very costly process as high pressure

and temperature is required for it. Comparatively, PODS has attained more attention due to low cost needs and high efficiency.

1.5.1 Hydrodesulfurization (HDS)

It is one of the techniques that is used for fuel desulfurization. In this technique, sulfur from fuel is converted into hydrogen sulphide gas in the presence of catalyst and is mostly applied in industries. Thiophenes are difficult to remove by using this technique, however, mercaptan and sulfides are extracted conveniently. This method is not appropriate for desulfurization of low fuel as it is costly and extremely high reaction conditions are required.¹⁴

1.5.2 Non-Hydrodesulfurization Procedures

Non-HDS procedure is an advanced method (Figure 1.2) that includes the adsorptive desulfurization, extractive desulfurization, bio-desulfurization, oxidative desulfurization and Photo-oxidative desulfurization in it.

Non-HDS processes are growing rapidly as they exhibit good ability to remove thiophenes than HDS process.¹⁵

1.5.2.1 Extraction Desulfurization (EDS)

In this technique, proper miscibility of extractant, that is used for sulfides removal, and sulfur containing fuel is highly needed. Usually a polar solvent is used for this purpose. Sulfur from fuel can be removed by multiple EDS techniques.^{16, 17}

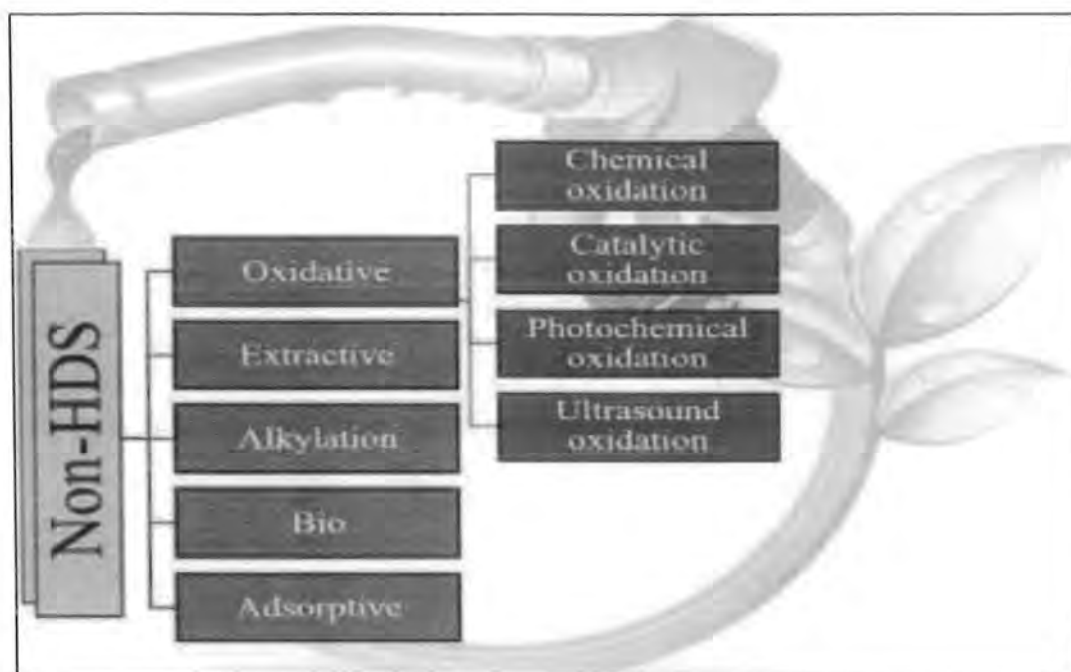


Figure 1.2 Non-hydrodesulfurization techniques.¹⁸

1.5.2.2 Bio Desulfurization (BDS)

In this process, enzymes or proper microbes are used to remove sulfur by converting non-polar sulfur organic compounds into polar compounds that are water soluble and then they are eliminated in a mild environment.

1.5.2.3 Adsorptive Desulfurization (ADS)

An appropriate adsorbent (solid) is used to adsorb and removal of the sulfur compounds present in the fuel. Major goal in this process is preparation and selection of a proper adsorbent such as zeolites, metal oxides etc.¹⁹

1.5.2.4 Oxidative Desulfurization (ODS)

ODS is a process in which sulfoxides and sulfones are formed by oxidation of sulfur in the catalyst presence and proceeded with extraction. The most crucial factor in this method is the selection of catalyst like organic acids, inorganic heteropoly acids and oxidant like molecular oxygen, ozone, and hydrogen peroxide.^{20, 21}

ODS process involves three major stages. Firstly, an oxidant is used to convert the sulfides into sulfoxides or sulfones which is followed by extraction. In the last, catalysts are recovered again.²²

The mechanism of ODS is explained as follow; at first the catalyst interact with the sulfur containing compound where sulfoxide is formed after the attack of oxygen atom on sulphur. Aromatic structure is destroyed here sulfone is formed quickly by oxidation of sulfoxide. Then an extractant is used to extract the sulfone. Thiophenes are degraded effectively by following this method.²³

1.5.2.5 Photo-Oxidative Desulfurization (PODS)

To combat numerous environmental contamination challenges, photocatalytic technology uses light irradiation to activate a photocatalyst and speed up the advancement of a chemical reaction. Advanced oxidation processes like photocatalysis have attracted a lot of interest. This process has gained a lot of attention because of high performance of catalyst and oxidant under light without harmful chemicals.²⁴⁻²⁶ The distinguishing qualities of this process are, it is environmentally friendly, easy to afford, non-complexity, operatable under mild reaction conditions and efficient transformation of toxic chemicals into eco-friendly materials.²⁷⁻²⁹

There are two main parts of PODS, the one in which oxidation of photocatalyst occur and the other in which the separation of sulfones takes place which are shown in Figure 1.3. Photocatalytic oxidation is done by introduction of feedstock that contain organosulfur compounds in the reactor and light is irradiated over it for photocatalyst activation as large amount of oxygen is present here. Sulfones and sulfoxides are formed, and they are extracted in the next zone and removed from the system.

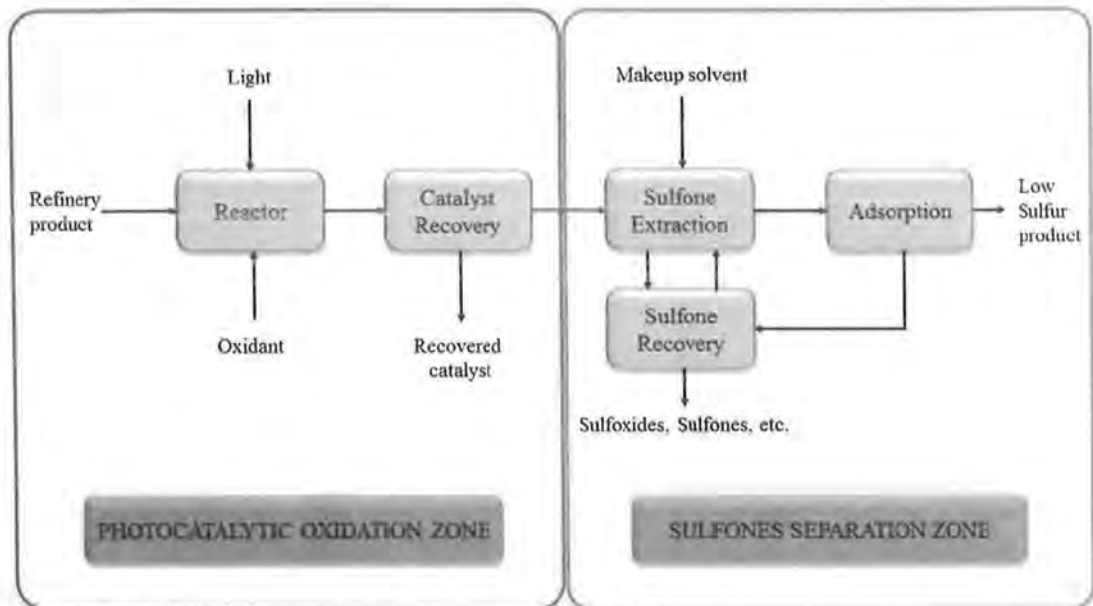


Figure 1.3 Simplified overview photo-oxidative desulfurization process.

Photo-Oxidative Desulfurization (PODS)

1.5.3 Catalytic Systems

1.5.3.1 Homogeneous Catalytic Systems

Homogeneous catalysis has greatly found its usage in fuels that contain larger amount of heavier sulfur containing organic compounds. In these catalytic systems different factors like oxidant quantity, reaction temperature and time of reaction are studied.²³

1.5.3.2 Heterogeneous catalytic systems

Heterogeneous catalysis is a process that is used for fuel that contains sulfur in variable portions. After the transformation of sulfides into sulfones, catalyst and product separated easily that's why this method is more preferable than homogeneous catalysis. A support is mostly used with metal-based catalyst for surface area increment which enhances the catalytic activity in heterogeneous catalysis.³⁰⁻³² The heterogeneous catalysis finds its major use in the ease of separation of catalyst and product.

1.5.4 Oxidizing agents used in PODS.

1.5.4.1 Organic peracids

The peracids are very reactive and cause corrosion which indicates that they are strong oxidizing agents.^{33, 34} As some fuels contain excessive amounts of sulfur, these oxidizing agents are used for successful oxidative desulfurization process which makes it quite costly. Furthermore, to ensure complete desulfurization, it is a prerequisite to use a metal based catalyst which remains stable in the presence of strong oxidizing agents.^{35, 36} For examples Peroxy acids, Peracetic acids.

The sacrificial aldehyde in the presence of oxygen is another reagent which can be used to oxidize the sulfur containing compounds in fuel but it is a weak oxidizing agent and even in the presence of a catalyst made of metal, it can't ensure full oxidative desulfurization.^{37, 38}

1.5.4.2 Organic hydroperoxides

Under the efficient catalytic presence, the organic hydroperoxides are used as oxidizing agents for oxidative desulfurization in sample reactor activity but they have some limitations as well. These oxidizing agents produce active oxygen in a very limited amount, some side reactions may also occur which decrease the catalytic activity significantly and they are not economical as well.

Two different processes are used to separate the sulfones which are produced by these oxidizing agents. The first one for removal of sulfones is extraction method is also known as Lyondell process while the second one is the adsorption method for sulfones removal i.e.; Eni Chem/UOP method.

1.5.4.3 Hydrogen peroxide

Hydrogen peroxide is the most propitious oxidizing agent and its major advantages to use is as an oxidant include that the mass of active oxygen increases by 47% without the formation of toxic by-products as only water is produced as a side

product.³⁹ To enhance the mass transfer by increasing the speed of reaction and to make it more commercial, heterogeneous catalyst is used.

1.5.5 Extraction in PODS

The sulfones and sulfoxides are formed through oxidation in PODS method from model oil in which the solvent is used that is immiscible and they are separated out through extraction.^{40, 41} The density difference between two solvents and polarity difference between the solvents affect the extraction efficiency greatly. To ensure the process of extraction more beneficial other solvent properties such as melting point, boiling point and surface tension are equally important in recovery and recycling of solvent. Through centrifuge the extractive solvent is isolated out.

1.5.5.1 Properties of solvent used for extraction.

To extract sulfones from hydrocarbons mixture, the selection of appropriate solvent has crucial significance. Various parameters are used for suitable solvent selection and it should be recovered easily. The less solubility of solvent in hydrocarbon mixture save it from fractional loss of solvent and various extractions are also required. For example, Acetonitrile, Dimethyl sulfoxides etc.

1.5.6 PODS Methods

1.5.6.1 Radiation assisted oxidation

Hydrogenation process which shows progress through induction of radiations is used to remove the compounds that contain sulfur and break the larger hydrocarbon molecules through the hydrogen production. Sulfur is mostly removed in the form of hydrogen sulfide gas. This process converts light sulfur compounds into sulfones and sulfur oxides and is efficient for their removal.⁴²

The process of irradiation consists of two main steps. First step involve the irradiation of compound and in the second step extraction method is used to remove the compounds that contain oxidized sulfur. However, compounds of sulfur are

removed in this method to a small extent, for their complete removal double oxidation method is preferred.

1.5.6.2 Ultrasound assisted ODS.

In this process ultrasound waves form an emulsion, which increase the interfacial area for the reaction to occur and results in the increment of reactants mass transfer to the interfacial area and speed up the rate of reaction.^{43, 44} Active species are produced due to sonication process which cause the high pressure and temperature and reaction will proceed fast.⁴⁵ Hence the ODS process that use the ultrasound waves that undergo phase transformation in catalyst presence is called ultrasound assisted ODS process.

1.5.6.3 Photo-oxidation

It is one of the most reliable method in which UV-Visible light source is used to remove the compounds that contain sulfur in fossil fuel such as thiophene and DBT. It consists of two major stages which include the oxidation of compounds that contain sulfur under UV-Visible light source and then the extraction of oxidized compound has done in presence of some polar solvent such as water or acetonitrile at room temperature and pressure.⁴⁶

1.5.6.4 Plasma ODS

Organic sulfides such as mercaptans and thiophenes are removed from organic sulfides through this method. This process has some limitations, it is not economical and even at higher pressure and temperature only the partial oxidation of compounds that contain sulfur usually occurs.⁴⁷

1.5.7 HDS and ODS Processes

1.5.7.1 HDS process

In today's world, sulfur containing compounds are removed from fossil fuel through a most commonly used method i.e; hydrodesulfurization (HDS). A metal-

based catalyst is mostly used in the process that convert the sulfur containing compounds into hydrogen sulfide gas which is toxic in nature.

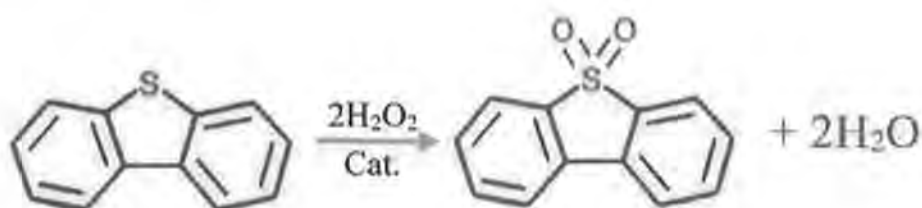
HDS process is quite costly due to the requirement of large reactors and extreme reaction conditions such as high temperature and pressure.

It is an adequate process for elimination of various compounds that contain sulfur such as thiophene, disulfides, mercaptans and sulfides but aromatic sulfur hydrocarbons cannot be eradicated from fossil fuel.

1.5.7.2 ODS process preference over HDS process

In 1960, ODS process was started but it gained significant importance in 1990s where extraction method and a proper oxidizing agent is used to remove the sulfur containing compounds from the fuel. The ODS process is preferred over HDS because of moderate reaction conditions i.e; low temperature and pressure. In ODS process, sulfones and sulfoxides are formed due to the oxidation of sulfur containing compounds under the presence of a catalyst, an oxidizing agent, and immiscible solvents, followed by the extraction of the oxidized compounds.

The oxidative desulfurization of Dibenzothiophene (DBT) occurs through following reaction.



In ODS process, the most competitive oxidizing reagent such as hydrogen peroxide is used due to multiple reasons such as ease of availability, environmentally friendly and less corrosive nature. Moreover, it is also economically feasible.^{48, 49}

1.5.7.3 Advantages of ODS process

ODS process has various utilities such as sulfur species can be eradicated more easily that were not removable with HDS. Inert atmosphere is not required in refineries, it needs moderate reaction conditions of temperature and pressure. This method is cost effective as in HDS expensive hydrogen gas is used. The compounds that contain sulfur can be easily removed by oxidation. Oxidation/extraction process is an adequate process to expunge the sulfur with lower octane number.

1.5.7.4 Disadvantages of ODS process

ODS process has some limitations as well. It is not used on the industrial scale as it requires enormous amount of chemicals which have lethal consequences in surroundings. The reported catalytic schemes are virulent, non-selective and costly due to which the fuel quality can be compromised, and per capita need of fuel is increased and that's not economical.

1.5.8 Importance of Desulfurization of Fuels

The desulfurization of petroleum fuels is necessary due to the following reasons.

1.5.8.1 Corrosion

On account of the presence of sulfur compounds, mercaptans, H_2S gas and disulfides corrosion can occur in the fuel sector. In different areas of petroleum industry, chances of corrosion are present i.e; manufacturing, transportation and purging operation.⁵⁰

1.5.8.2 Destruction and pollution of environment

Burning of organic fuels that contain sulfur and sulfur containing compounds produce the toxic sulfur oxides (SO_x) such as sulfur dioxide (SO_2) and sulfur trioxide (SO_3), however sulfur dioxide will be produced in larger amount. In humans these dangerous gases cause different diseases such as asthma and other respiratory disorders. Acid rain also occur due to the presence of sulfur oxides in atmosphere and

it has very harmful impacts on environment such as building material corrosion, damage to plants and deadly consequences on aquatic life because of water bodies acidification.⁵¹

1.5.8.3 Deactivation of catalysts

Catalyst deactivation happens in oil refining while desulfurization process due to the production of deadly gases like $\text{SO}_x/\text{NO}_x/\text{H}_2\text{S}$. Deactivation of catalyst mainly happen due to the presence of hydrogen sulfide and sulfur dioxide gas that will alter the selectivity and activity of catalyst.

1.5.9 Future Challenges to PODS

The major challenges for following PODS are to choose competitive oxidizing agent and to select the appropriate solvent.

Quality of fuel can be compromised because of the side reactions that may occur due to some oxidants. Picking up of right solvent is another challenge for extraction purpose of sulfur containing compounds as an inappropriate solvent do not extract all compounds that have sulfur and they also remove desirable aromatic compound from the fuel.⁵²

There are some significant pre-requisites for PODS process such as the oxidant choice, appropriate reaction conditions, selection of extractant and a catalyst that is cost effective for removal of sulfur containing compounds.

1.5.10 Improvements for PODS

PODS process has supremacy over all other processes because of many factors like low temperature and pressure requirements for reaction operation with oxidizing agents such as hydrogen peroxide with great efficacy. PODS process efficiency could be greatly improved by enhancing the particular catalytic activity even at low $\text{H}_2\text{O}_2/\text{S}$ ratios and by enlarging the mass movement inside a biphasic system that is comprised of polar phase (acetonitrile) and non-polar phase (oil).

1.5.11 Advantages of PODS

Advantages of PODS over alternative treatment options are its ease of use, low cost, sustainable technology, environmental friendliness, capability to perform at room temperature, and its great selectivity in the conversion of harmful pollutants into nontoxic compounds.^{27, 29, 53}

1.5.12 Basic Principle of PODS

PODS works on the photocatalytic principle in which holes (h^+) and electrons (e^-) are produced for fuel desulfurization under illumination of light as shown in Figure 1.4. In this method, production of charge carriers, their appropriate transmission and utilization takes place. When incident light contains the photon having energy equal or more than the photocatalyst band gap energy is interacted with photocatalyst, that photon beam gets absorbed on semiconductor surface and create holes in valence band due to the jumping of electrons from conduction band (CB) to valence band (VB).

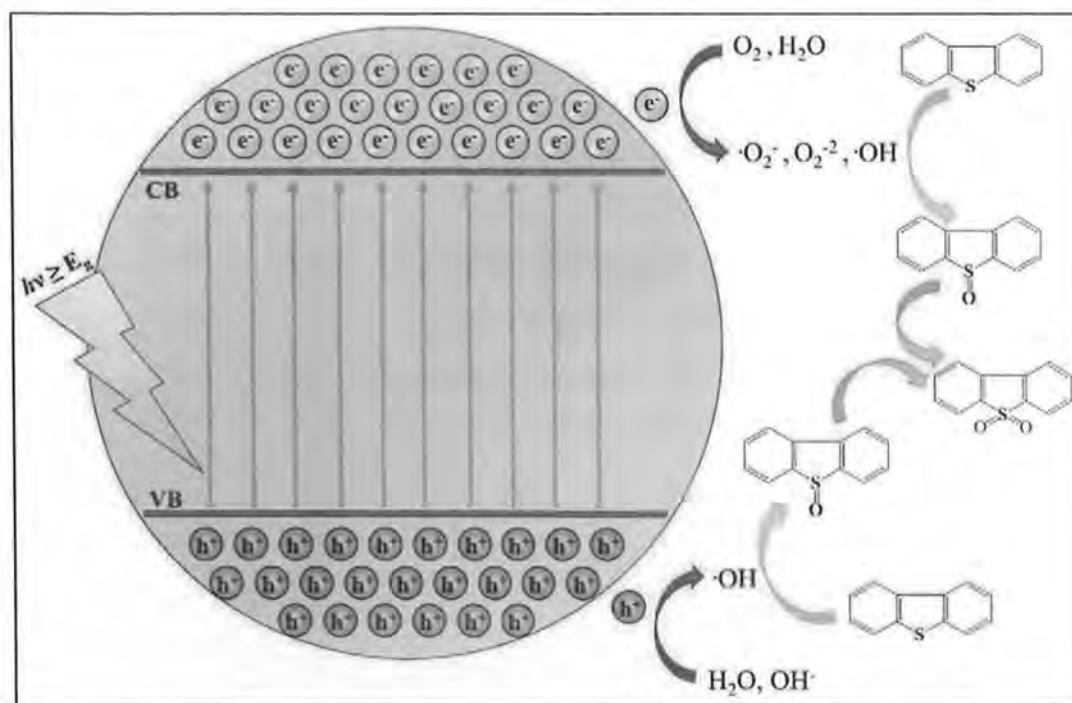
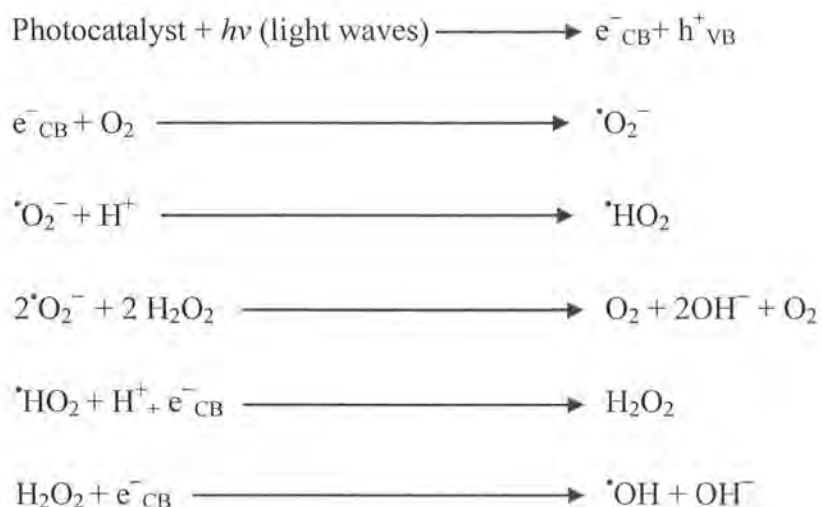
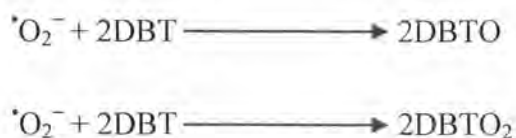


Figure 1.4 Schematic diagram of photo-oxidative desulfurization of liquid fuels.⁵⁴

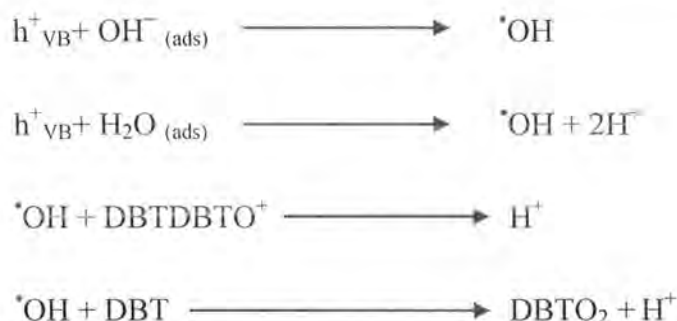
When electrons produced by photo irradiation reach the semiconductor photocatalyst surface and molecular oxygen (O_2) gain electrons to produce superoxide anion species/radicals ($O_2^{\cdot-}$, $O_2^{2\cdot-}$),^{55, 56} which further convert into OH^{\cdot} through a reactions series.⁵⁷ This sequence of reactions could involve the following interactions between the radicals of oxygen anion and the protons (H^+) on the surface or the hydroxide ions of the air-adsorbed water vapours.⁵⁸⁻⁶⁰



It is thought that along with the anionic radicals that generated through photons at the 2 and 5 carbon atoms of thiophene cycle, it is believed that this time period marks the beginning of the creation of the most unstable, reactive, and oxidised form of organo-sulfur compounds is based on thiophene.⁶¹ As a result, the photogenerated specie/radicals of superoxide anion ($O_2^{\cdot-}$, $O_2^{2\cdot-}$) have enough ability sulfur compounds oxidation to their respective sulfoxides and sulfones.⁶²



The photo generated holes either react with the adsorbed-water vapour in the atmosphere (H_2O) to produce radicals, OH^{\cdot} , or they acquire electrons that are generated from the organo-sulfur compounds and adsorbed on the semiconductor photocatalyst surface.⁶³ These reactive, unstable, and oxidised forms of thiophene-based sulfur compounds interact chemically with the OH^{\cdot} radicals and the photo generated holes to produce a number of oxidative reactions.⁶⁴⁻⁶⁶



The quick recombination of photo generated electron-hole pairs (Figure 1.5) continues to be the main obstacle in the production of semiconductor photocatalyst that is effective because of the high coulombic force that exists between these photo generated species. On the other hand, the presence of two lone pairs of electrons on the sulfur atom in organo-sulfur compounds made the hydroxyl radicals are more reactive than superoxide anions.^{62, 67} Therefore, the rate of hydroxyl radical production is very essential for the oxidation of organo-sulfur compounds. Recombination of photo generated species, which slows down the oxidation of the organo-sulfur molecule, is a simple way to prevent the formation of hydroxyl radicals. The excess of oxygen not only encourages the abundant production of hydroxyl and superoxide anions, but also inhibits the reuniting of electron-hole pairs. By functioning as an active electron trap, oxygen adsorption on the surface of the semiconductor photocatalyst effectively prevents the recombination of electron-hole.⁶⁸ As a result, the photo generated charges are quickly depleted, and the semiconductor photocatalyst's ability to recombine photo generated electron-hole pairs both on the surface and within the bulk is hindered.

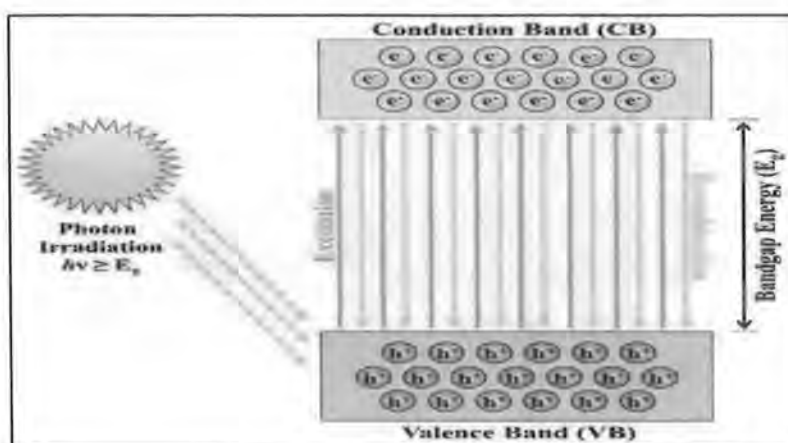


Figure 1.5 The photogeneration process of electron-hole pairs.⁵⁴

1.6 MXenes as a Co-catalyst

Researchers from Drexel University discovered innovative family of 2D materials in 2011. Recently, both theoretical and experimental chemists and physicists have shown a great deal of interest in a two-dimensional (2D) transition metal nitride/carbide family known as MXene. MXenes typically exhibit exceptional qualities, such as greater electrical conductivity, more chemical stability, and eco-friendly attributes, as a result of their distinctive structural characteristics. Studies revealed that, MXenes are used as potentially useful materials for semiconductors, lithium-ion batteries, super-capacitors, and hydrogen storage. Particularly, MXenes are effective materials for a variety of species due to their hydrophilic character and abundance of highly active surface terminations; as a result, these can be used for sensing or the elimination of environmental pollutants.⁶⁹

Due to its high surface area, adjustable chemistry, active surface functional groups, hydrophilicity, uniform structure, and chemical stability, MXene can be employed as an co-catalyst material to remove organic pollutants.

1.6.1 Structure of MXenes

The MXene are transition metal nitrides, carbides, and carbonitrides. Naturally, these are synthesized by selective etching of A layers from their parental materials, MAX phase ($M_{n+1}AX_n$), where M and A stands for initial transition metals such as Sc, Ti, V, Cr, Nb, Mo, Hf and a group IIIA or IVA element such as Al, Si. While X symbolizes C (carbon) and N (nitrogen).

H		M	A	X		He											
Li	Be	Early transition metal	Group A element	C and/or N	B	C	N	O	F	Ne							
Na	Mg				Al	Si	P	S	Cl	Ar							
K	Ca	Sc	Ti	V	Cr	Mn	Fe	Co	Ni	Cu	Zn	Ga	Ge	As	Se	Br	Kr
Rb	Sr	Y	Zr	Nb	Mo	Tc	Ru	Rh	Pd	Ag	Cd	In	Sn	Sb	Te	I	Xe
Cs	Ba	La	Hf	Ta	W	Re	Os	Ir	Pt	Au	Hg	Tl	Pb	Bi	Po	At	Rn

The MAX phase materials have value of $n = 1, 2, \text{ or } 3$. Therefore, MXenes are formulated as " $M_{n+1}X_nT_x$ ", where M and X are same as their parent material MAX phase, and " T_x " specifies surface termination groups like -F, -OH, -O which are produced through etching process.⁷⁰ There are three possible lattice structures of MXene such as M_2X , M_3X_2 , and M_4X_3 (Figure.1-6) as the n varies from 1 to 3 in the MAX phases. The first produced MXene was $Ti_3C_2T_x$.⁷¹

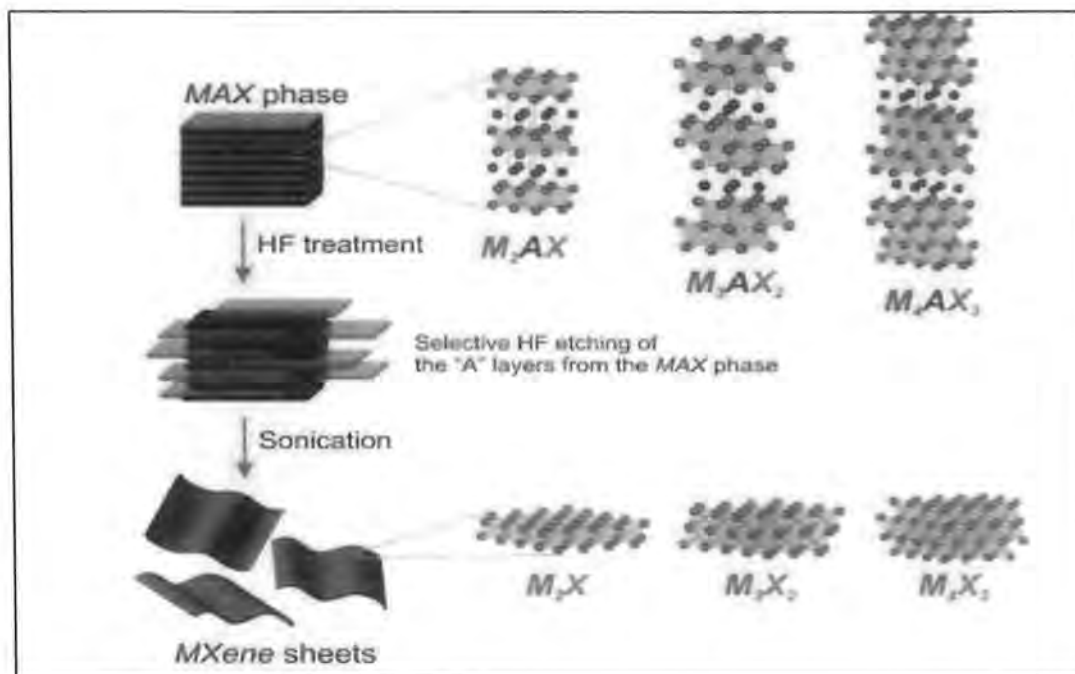


Figure 1.6 Structure of MAX phase and MXene⁷²

1.7 BiVO₄ as a Photocatalyst

Bismuth vanadate ($BiVO_4$) has been widely investigated because of its abundance, low cost, excellent photostability in aqueous solutions $BiVO_4$ is a non-toxic yellow pigment, and n-type semiconductors have a variety of fascinating technological characteristics, including ferroelasticity and ionic conductivity.⁷³ Due to its outstanding characteristics, which include a low band gap, resistance to corrosion, good dispersibility, non-toxicity, and an excellent photocatalytic result in the destruction of organic pollutants under visible light as shown in Figure 1.7, $BiVO_4$ has gained noticeably significant interest.⁷⁴



Figure 1.7 Properties/features of BiVO_4 nanoparticles

Additionally, its flexible optical and electrical characteristics with a band gap approximately 2.4 eV make it a strong choice for capturing solar radiation.^{75, 76} BiVO_4 exists in three major crystalline shapes such as, monoclinic scheelite phase (m-s), tetragonal zircon phase (t-z), and tetragonal scheelite phase (t-s). BiVO_4 nanoparticles can be produced readily using a variety of process like drop casting method,⁷⁷ hydrothermal,⁷⁸ co-precipitation method,⁷⁹ template free approach,⁸⁰ ultrasonication,⁸¹ mechanical milling,⁸² polymer assisted coprecipitation,⁸³ and sol gel,⁸⁴. Here, we discussed the state of the art in research on the environmentally friendly synthesis of BiVO_4 nanoparticles and their advantages over well-known traditional routes.

As a promising visible light photocatalyst, bismuth vanadate (BiVO_4) has a large pore size and high surface area, both of which are beneficial for enhancing the interaction of the catalyst active sites with the substrate and resulting in exceptional performance.⁸⁵

1.7.1 Drawbacks of BiVO_4

The lack of effectiveness of pure BiVO_4 as an adsorbent and the inefficiency of charge carrier separation as a photocatalyst limit its application.⁸⁶ Considering that, co-catalyst has been loaded onto BiVO_4 in order to increase the charge carriers separation.

1.8 Methods to Improve Photocatalytic Efficiency

It is crucial to increase the visible light activity of pure semiconductor materials in order to improve their photocatalytic performance. This can be done by altering the surfaces of the materials, such as by increasing their surface area, porosity, doping, or z-scheme, or by combining the photocatalyst with semiconductors that have a lower band gap. Alterations to the crystal structure caused by doping with metals, non-metals, dye sensitization, or the creation of heterostructures⁸⁷ can also decrease the probability of recombination.

1.9 Synthetic Methods for Photocatalyst

Photocatalyst can be synthesized by many advanced techniques. The following list includes some of the most popular techniques.

1. Co-precipitation
2. Sol-gel
3. Hydrothermal

The hydrothermal technique was used to make the BiVO₄/MXene composite.

1.9.1 Co-precipitation method

The most popular technique for creating nanoparticles and nanocomposites that separate the precipitates from the reaction's solution is called co-precipitation.

In order to get a homogeneous solution of ions, salts of divalent or trivalent metals are typically utilized as the initial component. These salts are dissolved in water or another suitable solvent, and one of the water-soluble salts undergoes a reaction. This water-insoluble salt then precipitates out in the form of oxalates or hydroxides when the species reaches the critical concentration needed to proceed on to the nucleation and growth phases. In addition to serving as precipitating agents, Na₂CO₃, NaOH, NH₃, or NH₄OH also work as reducing agents are used for maintaining the pH of solution.⁸⁸ The parameters that have a significant impact on the size and shape of the particles include the reaction medium's temperature, the

solution's pH and concentration, the type of base utilized, and the ratio of a chosen salt.⁸⁹ After the particles are precipitated, washed, and dried for further purification, the filtration or centrifugation is carried out. The particles produced with this approach exhibit less crystallinity. Therefore, calcination is carried out at high temperatures, and oxides are produced by this process from the hydroxides in order to increase crystallinity. After all impurities have been removed, these oxides are crystalline.⁹⁰

1.9.2 Sol-gel method

The sol-gel technique has increased in prominence as a useful method to synthesize new materials from molecular constituents while maintaining favourable reaction conditions for material modification.⁹¹ The sol-gel process yields a colloidal powder that, after being subjected to more heat, is transformed into a fine crystalline form.^{92, 93} Typically, the sol-gel method has been used to create nano and microstructures.

This method involves the simple wet process of hydrolyzing the metal alkoxide precursor in water or alcohol, the liquid phase (sol), which is created as a result of polycondensation in the presence of a base or an acid, is then changed into the condensed network known as a gel. The gel phase transforms into powder form as a result of the condensation of all the water molecules.

1.9.3 Hydrothermal Method

A well-established approach for the synthesis of various nanomaterials in a closed, high-pressure environment is the hydrothermal method. In a sealed container known as an autoclave, a hydrothermal reaction takes place at high pressure and temperatures between 100 and 250 °C.⁹⁴ The advantages of the hydrothermal approach include mild reaction conditions (temperature <300 °C), energy conservation, a one-step synthetic process, perfect and uniform doping, nucleation, environmental friendliness, and production of ultra-thin nanoparticles of high purity.⁹⁵ Figure 1.8 shows the stainless-steel autoclave, upper and lower discs, upper body, rod for locking and Teflon lining.



Figure 1- 8 Teflon lined autoclave.

1.10 Aim and Objectives of Research

The aims and objectives of this research are listed below:

- 1) To understand the chemical and photochemical properties of pure and modified BiVO_4 in nanostructured form. The modification involves composite formation.
- 2) To obtain nanoparticles of $\text{BiVO}_4/\text{MXene}$ nanocomposite using a simple hydrothermal technique.
- 3) To evaluate the structural, chemical, and photocatalytic characteristics of these synthesized nanoparticles.
- 4) To use $\text{BiVO}_4/\text{MXene}$ nanocomposite for PODS applications of DBT for Sulfur degradation.
- 5) To achieve a method that requires mild pressure and temperature conditions.
- 6) To develop an economical and environmentally friendly method for removing sulfur containing compounds from liquid fuels.

1.11 Plan of research

The objectives of the research are planned to be carried out in several parts. In the first part Pristine BiVO_4 , MXene and $\text{BiVO}_4/\text{MXene}$ will be prepared by hydrothermal method. Further, characterizations will be done to confirm successful synthesis. Afterwards, the photocatalytic activities would be checked by the degradation of sulfur compounds.

2 Experimental

2.1 Materials

2.1.1 Materials for synthesis of MXene

MAX phase i.e Ti_3AlC_2 99% provided by Nanoshel (UK) Ltd., hydrofluoric acid 48% provided by Unichem Sigma aldrich.

2.1.2 Materials for the Synthesis of Bismuth Vanadate

All chemicals and reagents were purchased from Sigma Aldrich, Fluka, Riedel-de Haën and E. Merck. Nitric acid (HNO_3), bismuth nitrate pentahydrate ($Bi(NO_3)_3 \cdot 5H_2O$), ammonium meta vanadate (NH_4VO_3), ethanol, sodium hydroxide ($NaOH$) and deionized water were used in the synthesis of bismuth vanadate. All the analytical grade chemicals were utilized without any further purification.

2.2 Synthesis

2.2.1 Synthesis of MXene

The MXene was synthesized by using 10mL of 48% hydrofluoric acid, per 1g of MAX phase Ti_3AlC_2 (98%). It was kept under stirring for 12h at $60^{\circ}C$. To obtain settled material, it was centrifuged for 10 minutes at 3000 rpm after being washed with DI water. The washing process was repeated multiple times until the pH was around 7. If it was still indicating acidic pH, the remaining acid was washed off by filtration because repeated centrifugation can cause delamination of MXene further complicating the separation. After drying for a night at $60^{\circ}C$, MXene was finally obtained. To obtain a few or single layer flakes as the end product of delamination, MXene was dispersed in water and subjected to ultrasonication for one hour.

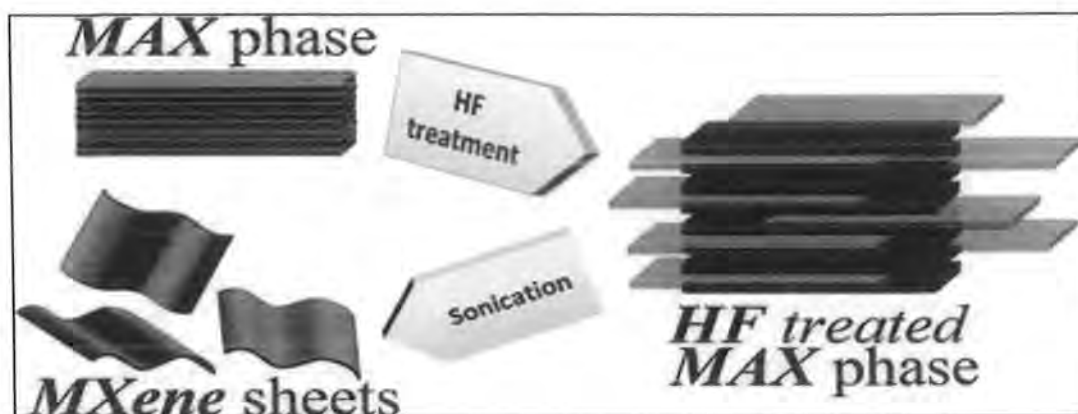


Figure 2.1 Synthesis scheme for MXene

2.2.2 Synthesis of Bismuth Vanadate

Bismuth vanadate nanoparticles were synthesized by facile hydrothermal method⁹⁶, as previously reported. Initially, two solutions were made labelled as solution A and solution B. Solution A was formed by dissolving 0.01 mol of $\text{Bi}(\text{NO}_3)_3 \cdot 5\text{H}_2\text{O}$ in 50 mL of 3 M nitric acid. Solution B was obtained by dissolving 0.01 mol of NH_4VO_3 in 50 mL of 2 M sodium hydroxide. Under continuous magnetic stirring, solution A was drop wise added to solution B. The pH of solution C was adjusted to 7 by adding required amount of 2 M NaOH solution and this solution was vigorously stirred for 1 hour. Then this catalyst precursor was poured into the autoclave Teflon lining and set of hydrothermal treatment for 18 hours at 180 °C. Autoclave was allowed to auto cool to room temperature and yellow precipitates of bismuth vanadate were obtained which were separated by vacuum filtration and washed multiple times with distilled water and ethanol. Finally, the product was dried at 80 °C for 12 hours as shown in Figure 2.2.

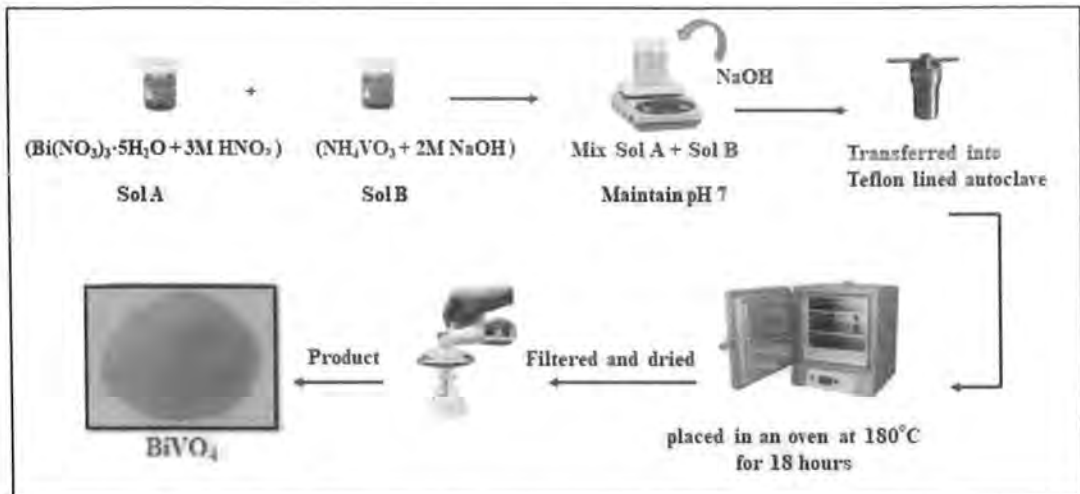


Figure 2.2 Synthesis scheme for bismuth vanadate

2.2.3 Synthesis of $\text{BiVO}_4/\text{MXene}$ composite

Same method was used for the synthesis of $\text{BiVO}_4/\text{MXene}$ composite as described in the section 2.2.2. 0.01 mol of bismuth vanadate and 0.01 mol MXene were added. Molar ratio of all other species were kept constant and sonicated MXene was added after neutralizing the pH of bismuth vanadate solution. Further steps i.e., hydrothermal treatment, filtration, washing and drying were performed at above mentioned conditions as shown in Figure 2.3.

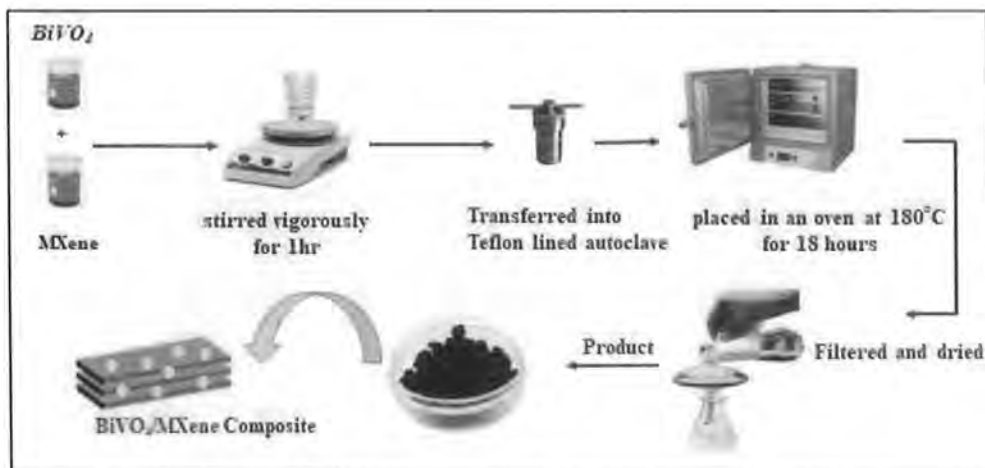


Figure 2.3 Synthesis scheme for $\text{BiVO}_4/\text{MXene}$ composite

2.3 Photo-Oxidative Desulfurization (PODS) of liquid fuel

DBT was dissolved in n-hexane to form a 500-ppm stock solution. From this stock, 50 ppm solution of dibenzothiophene in n-hexane (25 mL) was added with acetonitrile (25 mL). The PODS technique was carried out by adding a catalyst and an oxidizing agent (H_2O_2), and kept under light source, stirred it at various time intervals. Then, using a UV-visible spectrophotometer, the upper oily layer containing n-hexane and DBT was analysed. Once the equilibrium was attained, and the sulfur concentration in liquid fuel was estimated. At 284 nm, DBT exhibits a maximum absorption. By using thin layer chromatography (TLC), the sulfone production in acetonitrile was examined. The melting point of the resulting product ($229-232^\circ C$) proved that sulfones had been formed.

2.4 Photocatalytic Studies

Sulfur containing compounds were desulfurized with as-prepared photocatalysts under visible light to examine their effectiveness. The concentration of desulfurized compounds can be determined using a UV-Vis spectrophotometer. In this study, we also examined the effect of various parameters such as dose of catalyst, temperature, time and oxidant effect of solution on the degradation of DBT.

$$\text{Degradation Efficiency (\%)} = \frac{(C_0 - C_t)}{C_0} \times 100 \quad (2.1)$$

Where C_t , after time t concentration, and C_0 is initial concentration. Photo-Oxidative desulfurization efficiency is calculated by using equation 2.1.

Langmuir-Hinshelwood model was used in the determination of reaction kinetics. The following equation was used for the determination of rate constant and R^2 values.

$$\ln (C_t/C_0) = -k_{app} t \quad (2.2)$$

" k_{app} " signifies the rate constant for pseudo-first order reduction reaction and "t" is the time required for the completion of the reaction. Rate constant was measured from the slope of the graph plotted between $\ln (C_t/C_0)$ on the y-axis and t on the x-axis.

2.5 Procedure for Tauc Plot Calculations

UV-Vis spectra of MXene, BiVO₄, and BiVO₄/MXene composite were acquired by dispersing 0.01 g of catalyst into 50 mL of distilled water with the help of sonicator for ten minutes. The clear solution was proceeded to note UV-Vis readings and resulting data of all the samples were used to draw tauc plots.

2.6 Molar Absorbance Coefficient (ϵ)

Values of molar absorbance coefficient for DBT was calculating using Beer Lambert law, given below.

$$A = \epsilon \cdot l \cdot c \quad (2.3)$$

Where, A = Light absorbed by sample solution for given wavelength

ϵ = Molar absorptivity

l = Path length (distance travelled by light through solution)

c = Concentration per unit volume (of absorbing specie)⁹⁷

Solutions of DBT in n-hexane was prepared at different concentrations (10 ppm, 20 ppm, 30 ppm, 40 ppm and 50 ppm). Absorbance values of all the contaminants were taken at λ_{\max} of DBT for all the concentrations using spectrophotometer. Molar absorptivity (ϵ) was determined by conc. vs absorbance graph as shown in Figure 2.4.

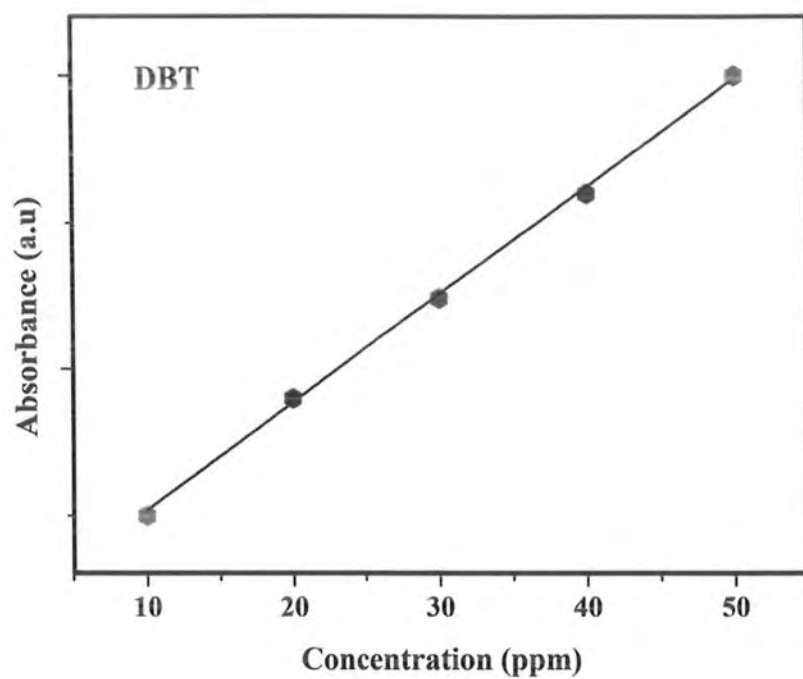


Figure 2.4 Calibration curve for DBT (λ max 284 nm).

3 Results and discussions

3.1 Characterization

To verify the composition, structure, and morphology of produced nanocomposites, a variety of analytical approaches have been used. i.e., energy dispersive X-ray spectroscopy (EDX), scanning electron microscopy (SEM) examination, and powder X-ray diffraction technique (PXRD).

3.1.1 X-Ray diffraction (XRD)

Using a powder diffractometer and a Cu- K α radiation detector with a wavelength of 0.154 nm and a scanning rate of 2°/min in the range of 2 θ from 20 to 70°, the Joint Committee on Powder Diffraction Standards (JCPDS) cards verified the results of powder X-ray diffraction (PXRD). The average particle sizes of nanoparticles less than 60 nm can be generally calculated using the Scherrer equation, which correlates the diffraction width (β) with the average particle size of the crystallite (D). The widening of the relevant X-ray spectral peaks was used to estimate the crystallite size. The sizes of the crystallites were determined by Scherer's equation using the sharpest peak's full width half maximum (FWHM).

$$D = K \lambda / (\beta \cos \theta) \quad (3.1)$$

Where K is the shape factor, λ is the employed X-ray wavelength, D is the average crystallite size in nm, and FWHM (full width half maxima) of the respective.

A BiVO₄/MXene composite crystal structure is identified by powder X-ray diffraction (P-XRD). The P-XRD data reveals that the monoclinic phase of BiVO₄ exhibits a pattern of sharp and narrow diffraction peaks (JCPDS 01-083-1699). The peak at 8.65° is associated with the (002) plane of MXene, which represents interlayer stacking as shown in Figure 3.1, while the peaks at 31.10°, 40.58°, 48.19°, and 53.69° are associated with the (004), (303), (204), and (301) crystallographic planes of

monoclinic crystal for BiVO_4 . The peak at 28.54° is the more intense peak, which is attributed to the (112) plane of BiVO_4 .

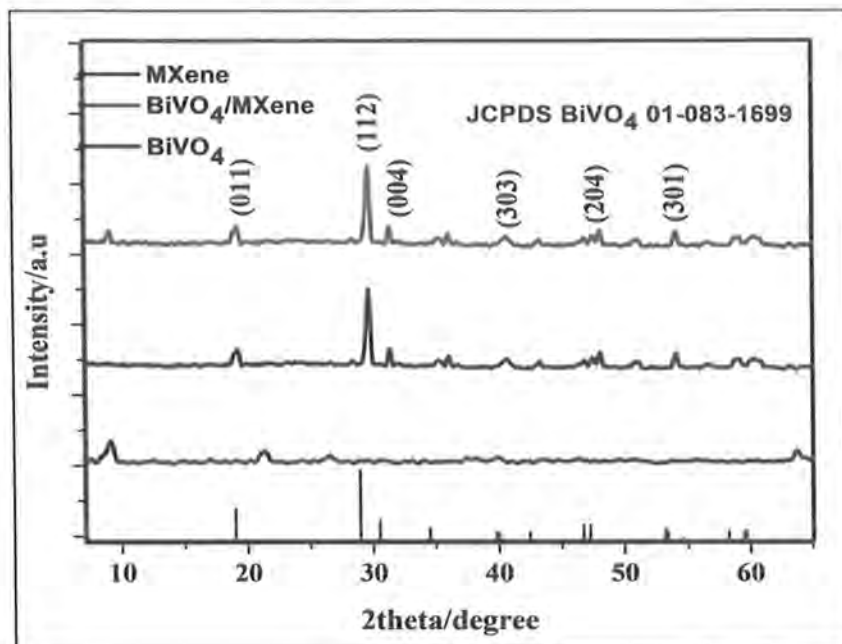


Figure 3.1 XRD patterns of BiVO_4 , MXene and $\text{BiVO}_4/\text{MXene}$ composite.

Similar diffractions to those of pure BiVO_4 were seen in $\text{BiVO}_4/\text{MXene}$ composite when MXene was used as a co-catalyst, demonstrating that the process had no effect on the crystal structure of BiVO_4 . Because the MXene layer was too thin and utilized as a co-catalyst, the diffraction of MXene in the $\text{BiVO}_4/\text{MXene}$ composite is invisible.

Table 3.1 Calculated crystallite size of synthesized photocatalysts

Photocatalysts	Crystallite size (nm)
BiVO_4	27.78
MXene	13.99
$\text{BiVO}_4/\text{MXene}$	20.90

3.1.2 Scanning electron microscopy (SEM)

A centred electron beam is scanned over a surface by a scanning electron microscope (SEM) to create an image. The interaction of the beam's electrons with the sample produces a variety of signals that can be utilized to gather information on the surface topography and composition. SEM (scanning electron microscopy) urges a ramification of signals at the surface of solid samples using a focussed stream of high energy electrons. Knowledge of the sample's external morphology (texture), crystalline structure, chemical composition, and orientation of its constituent materials, was disclosed by the signals that were reflected from electron-sample interactions. In the majority of applications, information was gathered across a specific area of the sample's surface, and a 2-dimensional image was made to show how these properties varied spatially.

To examine all the specifics of the morphology and particle size of the co-catalyst, SEM images of MXene were taken at various resolutions. SEM images of MXene show multilayer sheets having a large surface area to provide a catalyst activity place. SEM images of BiVO_4 was also taken at different resolution. SEM images of BiVO_4 show semi spherical shaped irregular nanoparticles having a large surface area to provide a catalyst activity site as shown in Figure 3.2. Whereas $\text{BiVO}_4/\text{MXene}$ composite shows that semi spherical shaped irregular nanoparticles of BiVO_4 stacked with MXene to give coral- reef like appearance which has great surface area and more porosity as shown in Figure 3.4.

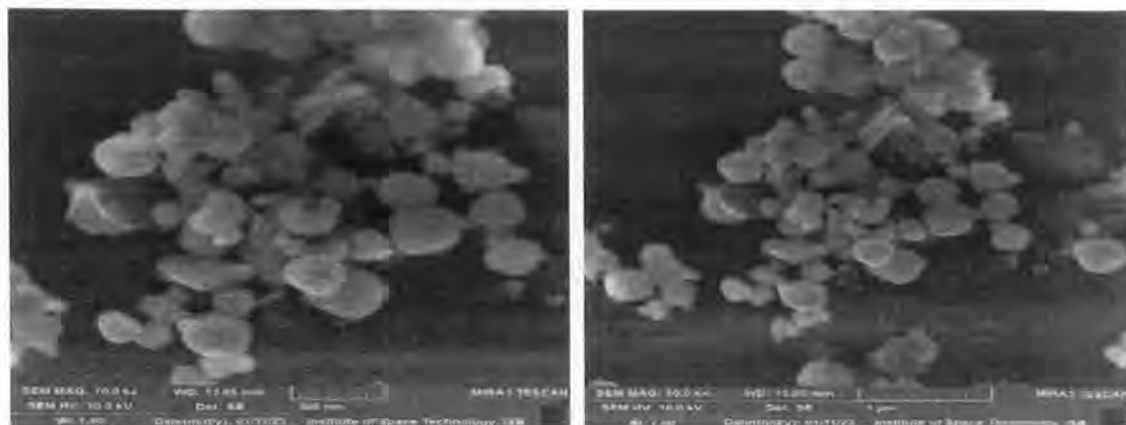


Figure 3.2 SEM images of BiVO_4 at different resolutions

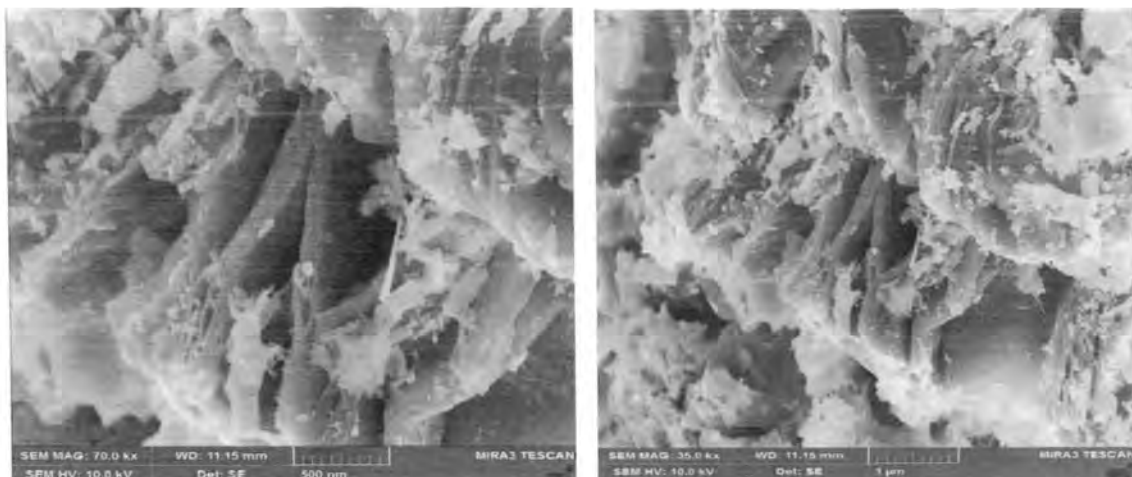


Figure 3.3 SEM images of MXene at different resolutions

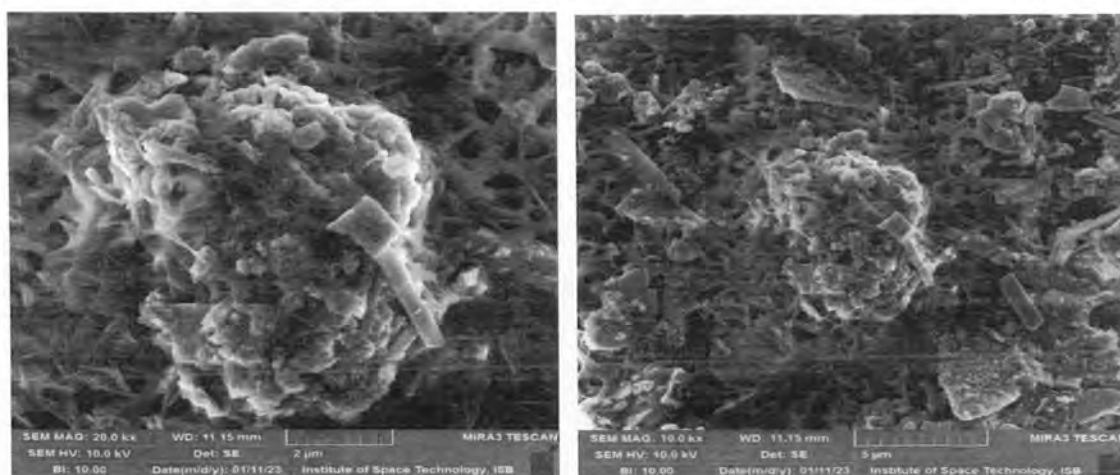


Figure 3.4 SEM images of BiVO₄ /MXene composite at different resolutions

3.1.3 Energy dispersive X-ray spectroscopy (EDX)

The EDX analysis, in which an X-ray beam interacts with the sample surface, is used to verify the catalyst's elemental composition. As a result, a specific set of peaks is generated based on the distinctive composition of each element. a combination of many elements that gave the catalyst its distinctive peak.

The presence of Ti, C, and O,F as terminating functional group elements is confirmed by the EDX spectra of MXene that the catalytic support material was successfully prepared as shown in Figure 3.5.

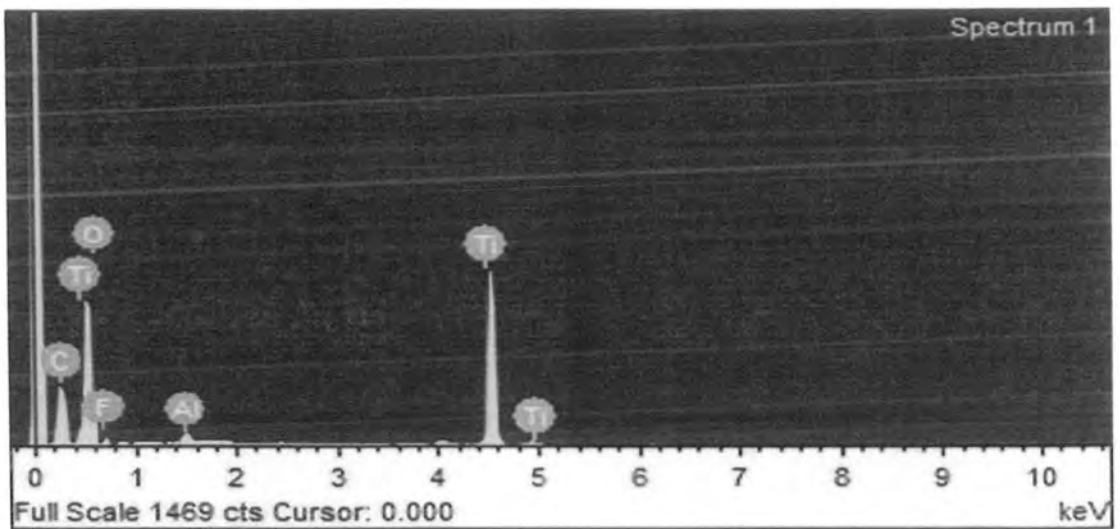


Figure 3.5 EDX analysis of MXene

The presence of the elements Bi, V, and O in the BiVO_4 EDX spectra indicates that the photo catalyst was successfully prepared as shown in Figure 3.6.

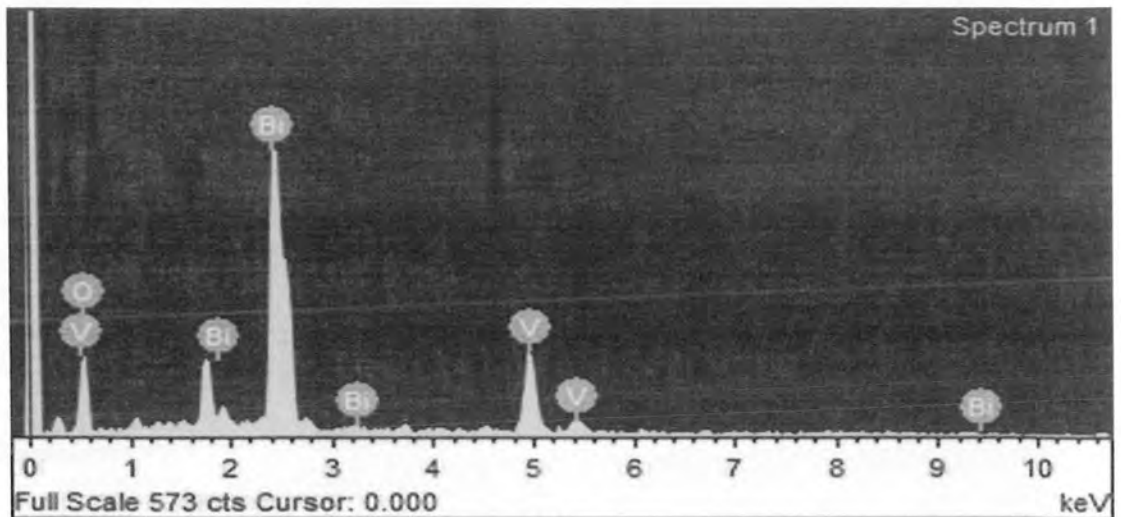


Figure 3.6 EDX analysis of BiVO_4

According to the EDX spectra of 15% $\text{BiVO}_4/\text{MXene}$ composite, the successful preparation of nano composite is confirmed by the existence of Bi, V, C, O, Ti and V elements as shown in Figure 3.7.

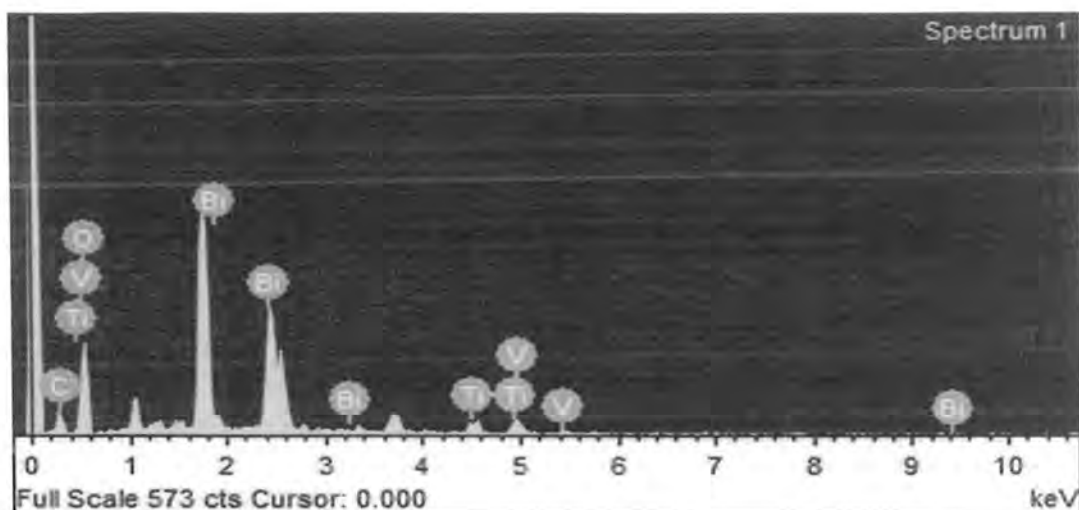


Figure 3.7 EDX analysis of BiVO₄/MXene composite

3.2 Optical Study and Band Gap Estimation

In semiconductor nano materials, transition of valance band electrons to the conduction band from valance band after absorbing an required amount of energy. Tauc equation is a mathematical expression for the the relationship between absorbance spectra and band gap energy, written as follows⁹⁸.

$$(\alpha h\nu) = k (h\nu - E_g)^n$$

Where, $h\nu$ = energy of photon

- n = type of transition ($n = 1/2$ for direct transition and $n = 2$ for indirect transition)
- k = tailing parameter (independent of energy)
- E_g = energy of band gap⁹⁹
- α = coefficient of absorption (calculated from Beer-Lambert law)

Extrapolation of linear region of plot $(\alpha h\nu)^2$ vs. energy ($h\nu$) gives the value of optical band gap, E.g. in UV-Vis wavelength range (200-800 nm). Several variables, including doping, grain size, and the kind of transition (direct or indirect), affect E_g values.¹⁰⁰. If electrons and holes possess the same crystal momentum in both conduction band and valance band, photon is emitted directly from electron, and then the band gap is termed as direct band gap. Whereas, in the indirect band gap until the

electrons cross an intermediate condition to provide momentum to the crystal lattice, photons are not released in the indirect band gap. The availability of oxygen vacancies can also lead to the formation of new states between the valance band and conduction band, decreasing the band gap. The band gap energies of BiVO_4 is 2.4-2.5 eV.¹⁰¹ The band gap energy of 15% $\text{BiVO}_4/\text{MXene}$ nanocomposite 1.98 eV as shown in Figure 3.8 and 3.9 respectively.

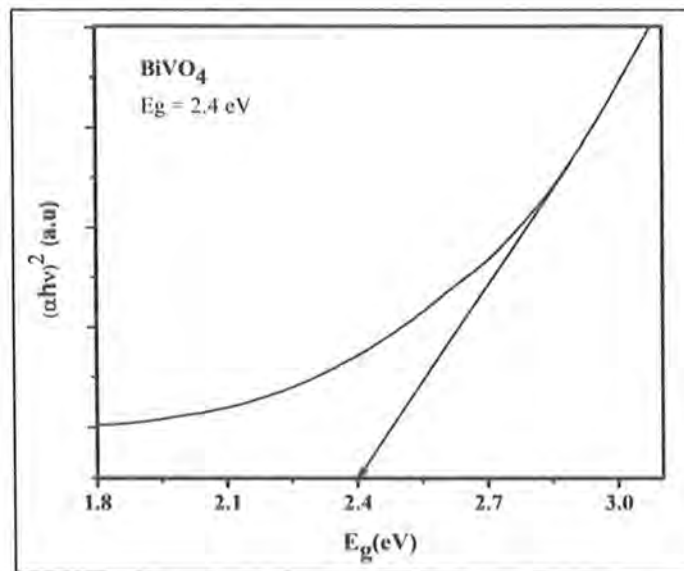


Figure 3.8 Tauc plot of BiVO_4

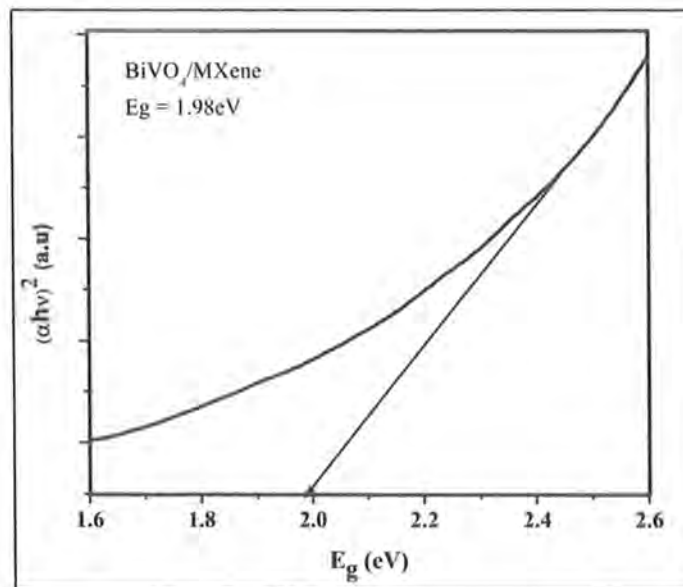


Figure 3.9 Tauc plot of $\text{BiVO}_4/\text{MXene}$

3.3 PODS studies.

3.3.1 Selection of Photocatalyst.

Using 30 mg of each photocatalyst and 30 mL of DBT in n-hexane solution (50 ppm), the photocatalytic activity of the samples as-prepared for the removal of sulfur was examined with a UV-Visible spectrophotometer. The resulting solution was irradiated under visible light for 1 hour on continuous magnetic stirring. Catalytic activity of the catalyst with and without support was shown on the graph. Due to the increased surface area and well-distributed catalyst on the support, which generates more active sites for reaction, the catalytic activity significantly increased by support addition. Without support, BiVO_4 removed sulphur containing compounds up to 49%, but when MXene was added, the removal of sulphur containing compounds was increased more than 90%. as shown in the Figures 3.10.

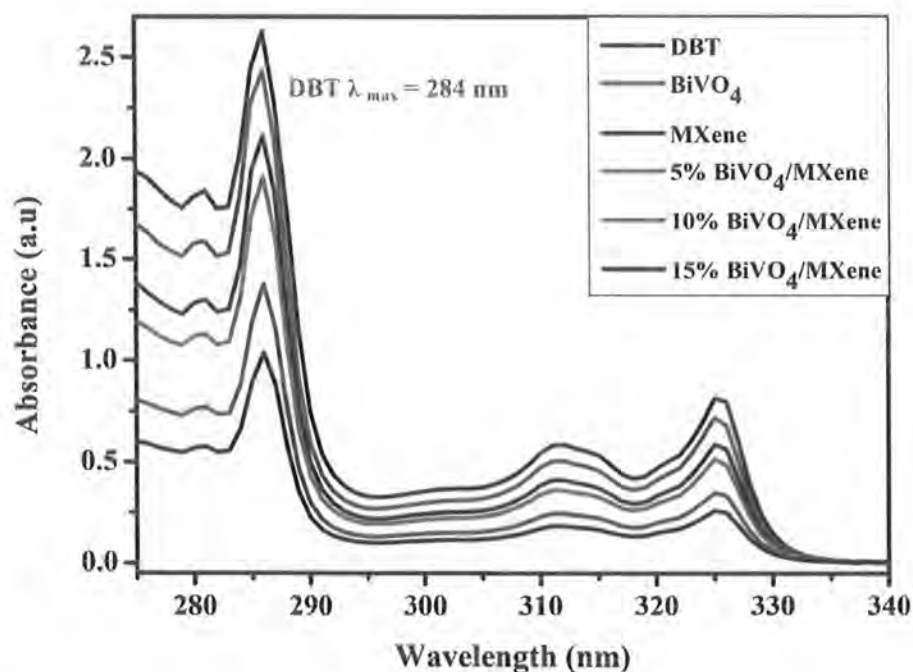


Figure 3.10 UV-Visible spectra of prepared catalysts for DBT degradation

3.3.2 Effect of time.

Removal of sulfur with 15% BiVO₄/MXene composite was examined for time optimization under visible light irradiation. The following conditions were used for the photo removal of sulfur experiment:

- **Time of irradiation:** 0-120 minutes
- **Amount of the catalyst:** 30 mg
- **H₂O₂ concentration:** 0.2 mL
- **Concentration of Liquid fuel:** kept constant at 50 ppm

With the passage of time, the transformation rate of sulfur containing compounds from sulfides to sulfones increased in a time period of two hours, all compounds containing sulfur removed. At time of 1.2hrs BiVO₄/MXene composite remove the sulfur up to 95% as shown by Figures 3.11. The same trend was observed for Fe₂W₁₈Fe₄@NiO@CTS hybrid nano catalyst and polysilicotungstate supported β cyclodextrin composite reported previously.^{12, 102}

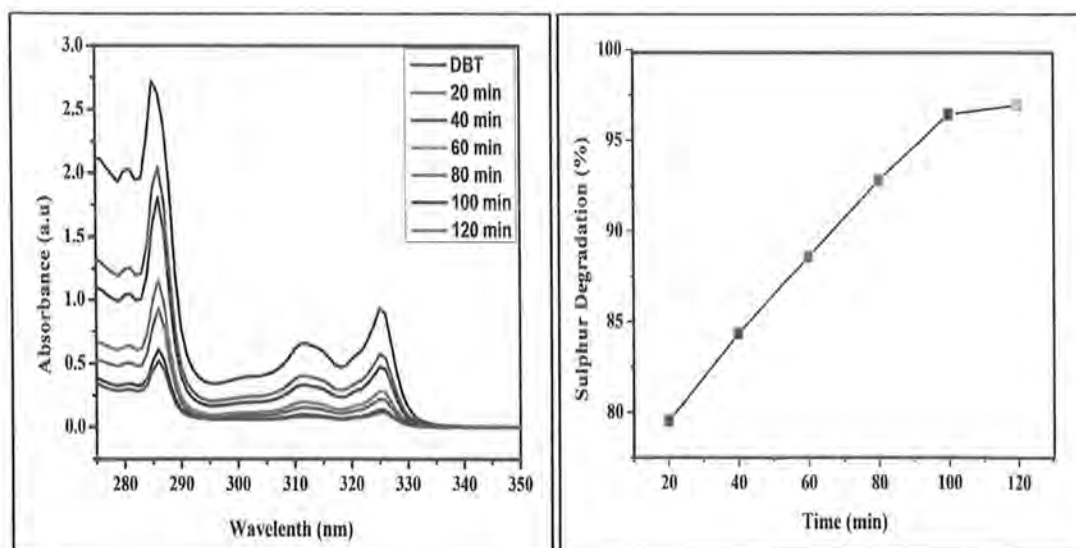


Figure 3.11 Effect of time on PODS process

3.3.3 Effect of catalyst dose.

It is worth important to know about appropriate amount of catalyst required for maximum efficiency not only for the estimation of cost, but also for the recovery of photocatalyst after degradation process. The catalyst dose has significant effect on

sulfur compounds elimination from liquid fuel. The following conditions were used for the photo removal of sulphur experiment:

- **Time of irradiation:** 100 minutes
- **Amount of the catalyst:** 10-60 mg
- **H₂O₂ concentration:** 0.2 mL
- **Concentration of liquid fuel:** kept constant at 50 ppm

The percentage of sulfur degradation increased along with the increment of catalyst dose from 10 mg to 60 mg. For better catalytic results, the optimum catalyst quantity was taken as 50 mg. By raising the amount of catalyst, the catalytic activity was enhanced greatly by increment in the catalyst amount as shown in the Figures 3.12 because of the availability of more active sites for catalytic activity to transform molecules containing sulfur into sulfones. The same trend was observed in case of Fe₂W₁₈Fe₄@NiO@CTS hybrid nano catalyst and polysilicotungstate supported β-cyclodextrin composite. According to the findings, catalyst amount and catalytic activity are directly correlated,

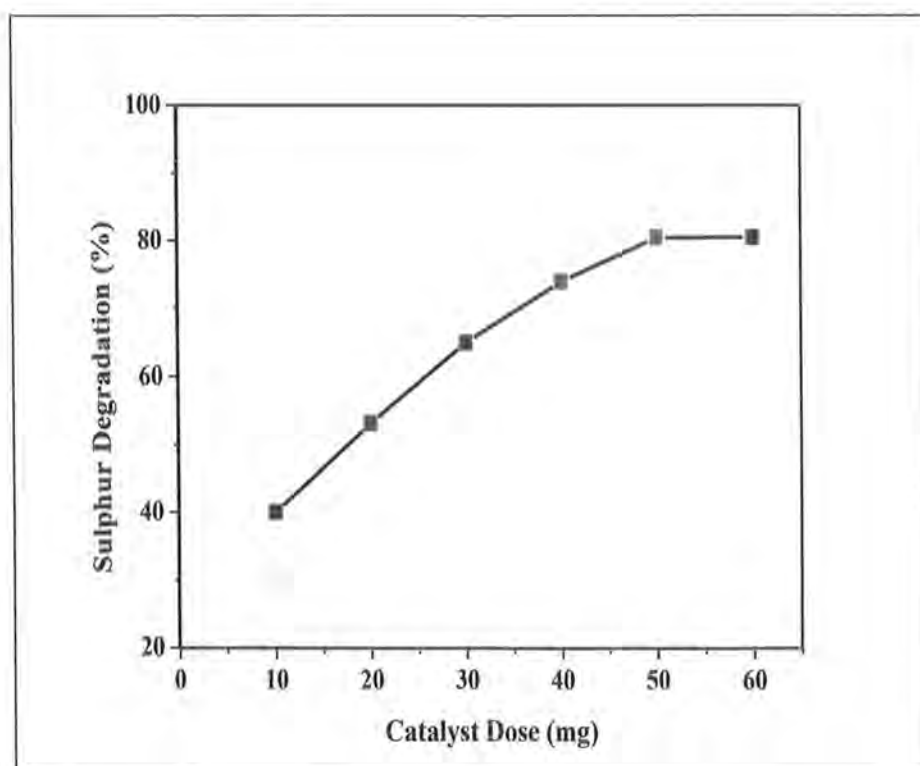


Figure 3.12 Effect of catalyst dose on PODS process

3.3.4 Effect of temperature.

The following conditions were used for the photo removal of sulphur experiment:

- **Time of irradiation:** 100 minutes
- **Amount of catalyst:** 50 mg
- **H₂O₂ concentration:** 0.2 mL
- **Concentration of liquid fuel:** kept constant at 50 ppm

The rise in temperature (up to 50°C) has accelerated the breakdown of sulfur compounds in liquid fuel. The ideal temperature for the best PODS result was taken as 50°C. Catalytic activity has increased as temperature has increased to a certain limit. The PODS process slows down at higher temperatures because H₂O₂ decomposition starts at higher temperatures, which slows down the photo-oxidative conversion of sulfides to sulfones. as shown in the Figures 3.13. Effect of temperature on percentage desulfurization was evaluated for WO₃/mesoporous ZrO₂, Fe₂W₁₈Fe₄@NiO@CTS hybrid nano catalyst show comparable result with BiVO₄/MXene.¹⁰³ which shows that the percentage degradation of sulfur increases when we increase temperature up to 50 °C.

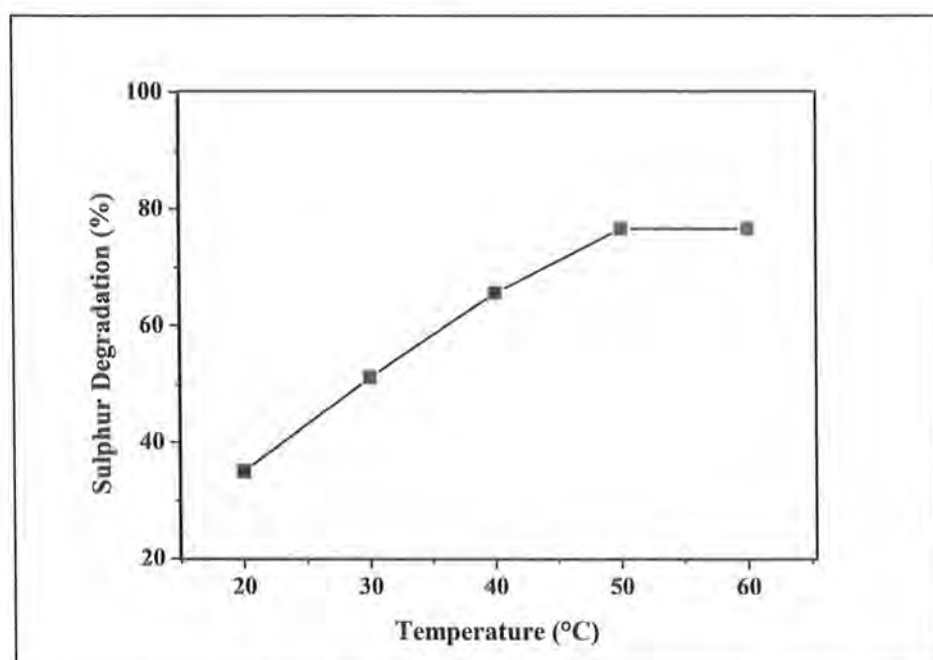


Figure 3.13 Effect of temperature on PODS process

3.3.5 Effect of hydrogen peroxide (H₂O₂).

The experiment was conducted under the following conditions:

- **Time of irradiation:** 100 minutes
- **Amount of catalyst:** 50 mg
- **H₂O₂ concentration:** 0.2-1 mL
- **Temperature:** 50°C
- **Concentration of liquid fuel:** kept constant at 50 ppm

The increase of oxidizing agent enhanced the PODS process. As shown in Figure 3.14, the PODS increases as the amount of H₂O₂ (an oxidising agent) is increased, but H₂O₂ can be used up to a specific limit. In the presence of the specified catalyst, 0.8 mL of hydrogen peroxide is the optimum amount to utilize for PODS. Because a higher H₂O₂ concentration can lead to self-decomposition, which would be ineffective for oxidative conversion, and it will be no further affected by increasing H₂O₂ amount. These results are comparable with some other catalysts such as [P₂W₁₈O₆₂]⁶⁻ and [P₅W₁₀O₄₀].^{13, 104}

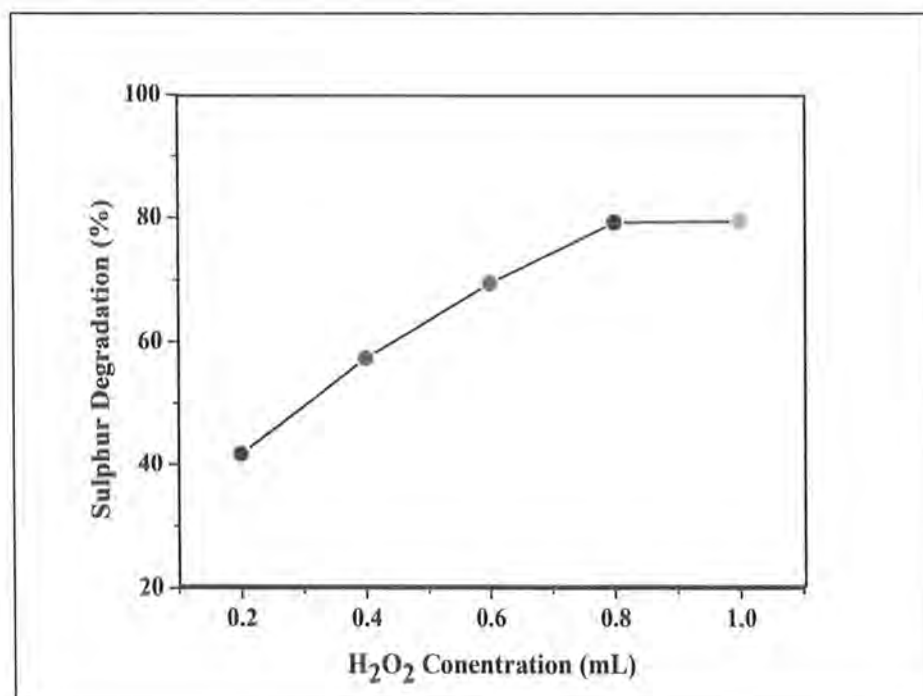


Figure 3.14 Effect of Hydrogen peroxide (H₂O₂) on PODS process

3.4 The kinetic studies for photo-oxidative desulfurization (DBT).

Reaction kinetics can be used to calculate the reaction rate. The reaction's rate constant is determined using the equation shown below.¹⁰⁵

$$\ln (C_0/C) = kt$$

In the upper oily layer of the reaction mixture, DBT and n hexane are present, while in the lower, catalyst and an oxidant are present. The results showed that the pseudo-first order kinetics of photo-oxidative desulfurization, which has a rate constant 0.029 min^{-1} and R^2 value is 0.989 and at $50 \text{ }^\circ\text{C}$, a straight line develops between $\ln C_0/C_t$ and the reaction's time (t) as shown in Figure 3.15. The trend shows the better result as compared to other metal-based catalysts such as $\text{PMoCu}@MgCu_2O_4\text{-PVA}$ composite and $\text{Fe}_2\text{W}_{18}\text{Fe}_4@\text{NiO}@\text{CTS}$.¹⁰⁶

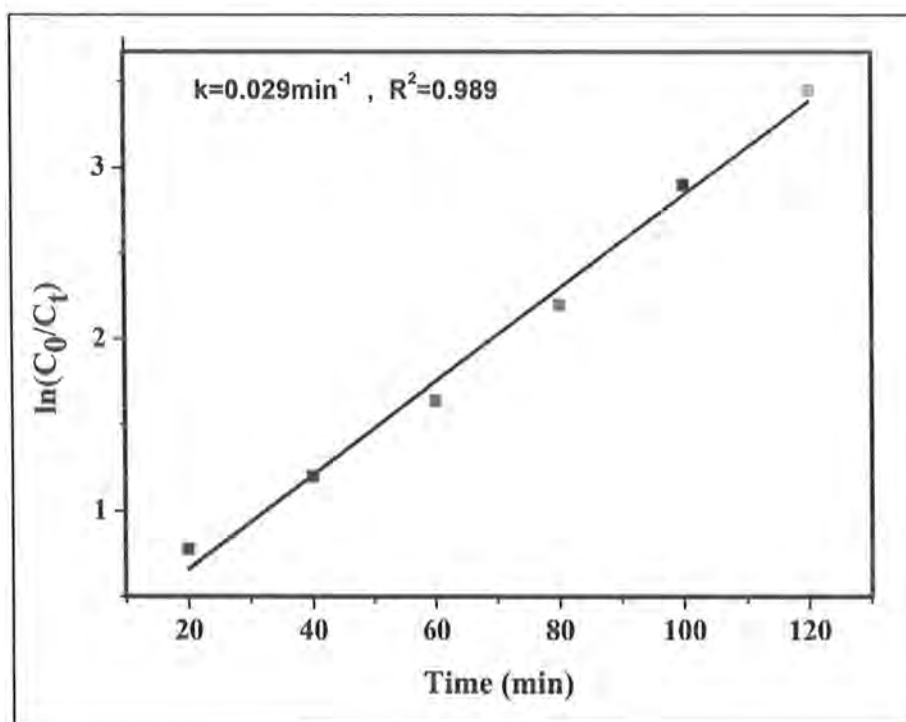
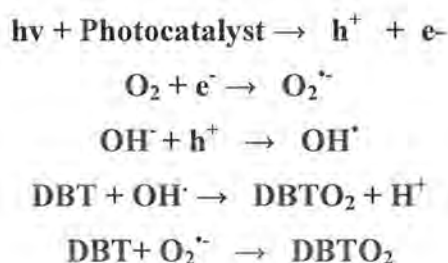


Figure 3.15 Kinetics of PODS process

3.5 Possible Mechanism for the PODS of Liquid Fuel.

Holes and superoxide anion radicals are responsible for the removal of sulfur from DBT. Holes and electrons are created when light strikes the photocatalyst's surface. While holes react with the hydroxyl ions to produce hydroxyl radicals, electrons react with the absorbed oxygen to form superoxide anion radicals. Only holes and superoxide anion radicals interact with DBT to cause removal of sulfur from liquid fuel.



3.6 Comparative study

According to the analysis of metal-based catalysts, these synthesised catalysts performed well when sulfur was removed from fossil fuels using the photo-oxidative desulfurization process. $CeO_2/g-C_3N_4$, $TiO_2/g-C_3N_4$, $SO_4^{2-}-TiO_2/RuO_2$, $C/TiO_2/MCM-41$, $ZnO/FSM-16$ composites have all been made and used to remove sulfur from fuel oil under visible light photocatalysis. Compared to our photocatalyst, these composites had less photocatalytic efficiency. With an efficiency of more than 95%, the $BiVO_4/MXene$ composite has shown good results for the removal of sulfur. Hydrogen peroxide was employed as the oxidising agent and DBT was used in n-hexane as the model fuel at a temperature of $50^\circ C$ for two hours. The results showed that, compared to the composite employed in this investigation, the catalyst was only able to extract sulfur to a maximum of 49% without support. The removal of sulfur was 95% from the fuel oil. $BiVO_4/MXene$ composite has revealed exceptionally good results in the catalytic photo-oxidative desulfurization of sulfur-containing molecules from the model oil due to the catalyst's higher surface area and greater efficiency as compared to other metal-based catalysts. This is because only 0.8 mL H_2O_2 and 50 mg of catalyst are required to completely remove sulfur from fuels, which is much less than other catalytic systems, as illustrated in Table 3-2.

Table 3.2 Comparison of desulfurization of liquid fuel by the PODS from the literature

Sr No.	Catalyst support	Catalyst Amount (g)	[DBT] n (ppm)	Light source	H ₂ O ₂ (mL)	DBT removal (%)	Ref
1	CeO ₂ g-C ₃ N ₄	0.2	500	300 W xenon lamp (visible light)	-	98	107
2	TiO ₂ g-C ₃ N ₄	0.2	500	250 W high pressure Hg lamp (UV light).	-	98.9	108
3	Ti ₃ C ₂ g-C ₃ N ₄	No data	500	A built-in xenon lamp (visible light)	-	99	85
4	SO ₄ ²⁻ -TiO ₂ RuO ₂	1	600	300 W high-pressure mercury lamp (visible light)	-	88	109
5	C/TiO ₂ MCM-41	1.5	300	300 W tungsten lamps (visible light)	-	95.6	110
6	ZnO FSM-16	0.3	200	Hg lamp (60 W, UV)	1	95	111
7	BiVO ₄ Ti ₃ C ₂ T _x	0.05	50	100 W Visible light	0.8	95	In this work

4 Conclusions

BiVO₄/MXene composite was successfully synthesized by hydrothermal method for the decomposition of sulfur containing compounds in the fossil fuels. Under moderate reaction conditions, the catalysts exhibited great efficiency in the photo-oxidation of DBT. MXene was used as a cocatalyst, which increased porosity, surface area, crystallinity, and active sites, and was attributed with the catalysts' excellent catalytic activity results. By optimising the reaction parameters, 50 mg of catalyst, 0.8 mL of hydrogen peroxide as the oxidant, 50 °C for the reaction temperature, and 2 hours of reaction time the removal rate of DBT from oil was increased by up to 95%. With an apparent rate constant of 0.029 min⁻¹ (R² = 0.989) for the interaction between BiVO₄/MXene, the kinetics investigations demonstrated that the reaction was pseudo-first order. This research showed that the PODS system has excellent catalytic activity for enhancing the quality of liquid fuel.

References

1. Fadhel, Z. S., Desulfurization of light diesel fuel using chloramine T and polymer supported imidation agent. *University of Technology, Iraq* **2010**.
2. Katzer, J. R.; Ramage, M. P.; Sapre, A. V., Petroleum refining: poised for profound changes. *Chemical Engineering Progress* **2000**, *96* (7), 41-51.
3. Babich, I.; Moulijn, J., Science and technology of novel processes for deep desulfurization of oil refinery streams: a review. *Fuel* **2003**, *82* (6), 607-631.
4. Chen, L.-J.; Li, F.-T., Oxidative desulfurization of model gasoline over modified titanium silicalite. *Petroleum Science and Technology* **2015**, *33* (2), 196-202.
5. Zhao, H.; Baker, G. A.; Zhang, Q., Design rules of ionic liquids tasked for highly efficient fuel desulfurization by mild oxidative extraction. *Fuel* **2017**, *189*, 334-339.
6. Bakar, W. A. W. A.; Ali, R.; Kadir, A. A. A.; Mokhtar, W. N. A. W., Effect of transition metal oxides catalysts on oxidative desulfurization of model diesel. *Fuel Processing Technology* **2012**, *101*, 78-84.
7. Subhan, S.; Rahman, A. U.; Yaseen, M.; Rashid, H. U.; Ishaq, M.; Sahibzada, M.; Tong, Z., Ultra-fast and highly efficient catalytic oxidative desulfurization of dibenzothiophene at ambient temperature over low Mn loaded Co-Mo/Al₂O₃ and Ni-Mo/Al₂O₃ catalysts using NaClO as oxidant. *Fuel* **2019**, *237*, 793-805.
8. Fox, B. R. Investigations into the oxidative desulfurization activity in a film-shear reactor, the source of enhanced reactivity, and other potential applications. University of Oregon, 2011.
9. Clemons, J. L., Adsorptive Desulfurization of Liquid Transportation Fuels Via Nickel-based Adsorbents for Fuel Cell Applications. **2009**.
10. Cheng, S. S. Ultra clean fuels via modified UAOD process with room temperature ionic liquid (RTIL) & solid catalyst polishing. University of Southern California, 2008.
11. Yu, F.; Wang, R., Deep oxidative desulfurization of dibenzothiophene in simulated oil and real diesel using heteropolyanion-substituted hydrotalcite-like compounds as catalysts. *Molecules* **2013**, *18* (11), 13691-13704.

12. Rezvani, M. A.; Imani, A., Ultra-deep oxidative desulfurization of real fuels by sandwich-type polyoxometalate immobilized on copper ferrite nanoparticles, $\text{Fe}_6\text{W}_{18}\text{O}_{70} \subset \text{CuFe}_2\text{O}_4$, as an efficient heterogeneous nanocatalyst. *Journal of Environmental Chemical Engineering* **2021**, *9* (1), 105009.
13. Hossain, M. N.; Park, H. C.; Choi, H. S., A comprehensive review on catalytic oxidative desulfurization of liquid fuel oil. *Catalysts* **2019**, *9* (3), 229.
14. Wu, N.; Li, B.; Ma, W.; Han, C., Synthesis of lacunary polyoxometalate encapsulated into hexagonal mesoporous silica and their catalytic performance in esterification. *Microporous and Mesoporous Materials* **2014**, *186*, 155-162.
15. Rang, H.; Kann, J.; Oja, V., Advances in desulfurization research of liquid fuel. *Oil Shale* **2006**, *23* (2), 164-176.
16. Zhai, L.; Zhong, Q.; He, C.; Wang, J., Hydroxyl ammonium ionic liquids synthesized by water-bath microwave: Synthesis and desulfurization. *Journal of Hazardous Materials* **2010**, *177* (1-3), 807-813.
17. Shiraishi, Y.; Tachibana, K.; Hirai, T.; Komasaawa, I., Desulfurization and denitrogenation process for light oils based on chemical oxidation followed by liquid-liquid extraction. *Industrial & Engineering Chemistry Research* **2002**, *41* (17), 4362-4375.
18. Haghghi, M.; Gooneh-Farahani, S., Insights to the oxidative desulfurization process of fossil fuels over organic and inorganic heterogeneous catalysts: advantages and issues. *Environmental Science and Pollution Research* **2020**, *27*, 39923-39945.
19. Song, C., New approaches to deep desulfurization for ultra-clean gasoline and diesel fuels: an overview. *Prepr Pap Am Chem Soc Div Fuel Chem* **2002**, *47* (2), 438-444.
20. Fedorova, E.; Zhirkov, N.; Tarakanova, A.; Ivanov, A.; Senyavin, V.; Anisimov, A.; Tulyakova, E.; Surin, S., Oxidative desulfurization of diesel fuel with hydrogen peroxide in the presence of vanadium peroxo complexes. *Petroleum Chemistry* **2002**, *42* (4), 253-256.
21. De Angelis, A.; Pollesel, P.; Molinari, D.; Parker, W. O. N.; Frattini, A.; Cavani, F.; Martins, S.; Perego, C., Heteropolyacids as effective catalysts to obtain zero sulfur diesel. *Pure and Applied Chemistry* **2007**, *79* (11), 1887-1894.

22. Craven, M.; Xiao, D.; Kunstmann-Olsen, C.; Kozhevnikova, E. F.; Blanc, F.; Steiner, A.; Kozhevnikov, I. V., Oxidative desulfurization of diesel fuel catalyzed by polyoxometalate immobilized on phosphazene-functionalized silica. *Applied Catalysis B: Environmental* **2018**, *231*, 82-91.
23. Wei, S.; He, H.; Cheng, Y.; Yang, C.; Zeng, G.; Qiu, L., Performances, kinetics and mechanisms of catalytic oxidative desulfurization from oils. *RSC advances* **2016**, *6* (105), 103253-103269.
24. Hauchecorne, B.; Lenaerts, S., Unravelling the mysteries of gas phase photocatalytic reaction pathways by studying the catalyst surface: a literature review of different Fourier transform infrared spectroscopic reaction cells used in the field. *Journal of Photochemistry and Photobiology C: Photochemistry Reviews* **2013**, *14*, 72-85.
25. Pawar, R.; Lee, C. S., *Heterogeneous nanocomposite-photocatalysis for water purification*. William Andrew: 2015.
26. Hosseini, A.; Faghihian, H.; Sanati, A. M., Elimination of dibenzothiophene from transportation fuel by combined photocatalytic and adsorptive method. *Materials Science in Semiconductor Processing* **2018**, *87*, 110-118.
27. Wang, H.; Wu, Y.; Feng, M.; Tu, W.; Xiao, T.; Xiong, T.; Ang, H.; Yuan, X.; Chew, J. W., Visible-light-driven removal of tetracycline antibiotics and reclamation of hydrogen energy from natural water matrices and wastewater by polymeric carbon nitride foam. *Water research* **2018**, *144*, 215-225.
28. Jusoh, N. W.; Jalil, A. A.; Triwahyono, S.; Karim, A.; Salleh, N.; Annuar, N.; Jaafar, N.; Firmansyah, M.; Mukti, R.; Ali, M., Structural rearrangement of mesostructured silica nanoparticles incorporated with ZnO catalyst and its photoactivity: Effect of alkaline aqueous electrolyte concentration. *Applied Surface Science* **2015**, *330*, 10-19.
29. Jalil, A.; Satar, M.; Triwahyono, S.; Setiabudi, H.; Kamarudin, N.; Jaafar, N.; Sapawe, N.; Ahamad, R., Tailoring the current density to enhance photocatalytic activity of CuO/HY for decolorization of malachite green. *Journal of Electroanalytical Chemistry* **2013**, *701*, 50-58.
30. Jiang, Z.; Hongying, L.; ZHANG, Y.; Can, L., Oxidative desulfurization of fuel oils. *Chinese Journal of Catalysis* **2011**, *32* (5), 707-715.

31. Ratnasamy, P.; Srinivas, D., Active sites and reactive intermediates in titanium silicate molecular sieves. *ChemInform* **2004**, *35* (50), no-no.
32. Long, Z.; Yang, C.; Zeng, G.; Peng, L.; Dai, C.; He, H., Catalytic oxidative desulfurization of dibenzothiophene using catalyst of tungsten supported on resin D152. *Fuel* **2014**, *130*, 19-24.
33. Otsuki, S.; Nonaka, T.; Takashima, N.; Qian, W.; Ishihara, A.; Imai, T.; Kabe, T., Oxidative desulfurization of light gas oil and vacuum gas oil by oxidation and solvent extraction. *Energy & fuels* **2000**, *14* (6), 1232-1239.
34. Ali, S. H.; Hamad, D. M.; Albusairi, B. H.; Fahim, M. A., Removal of dibenzothiophenes from fuels by oxy-desulfurization. *Energy & fuels* **2009**, *23* (12), 5986-5994.
35. Al-Shahrani, F.; Xiao, T.; Llewellyn, S. A.; Barri, S.; Jiang, Z.; Shi, H.; Martinie, G.; Green, M. L., Desulfurization of diesel via the H₂O₂ oxidation of aromatic sulfides to sulfones using a tungstate catalyst. *Applied Catalysis B: Environmental* **2007**, *73* (3-4), 311-316.
36. Hao, L.; Benxian, S.; Zhou, X., An improved desulfurization process based on H₂O₂/formic acid oxidation system followed by liquid-liquid extraction. Part 1. Coker gas oil feedstocks. *Petroleum Science and Technology* **2005**, *23* (7-8), 991-999.
37. Murata, S.; Murata, K.; Kidena, K.; Nomura, M. In *Oxidative desulfurization of diesel fuels by molecular oxygen*, Abstr Paper Am Chem Soc, 2003; pp U532-U532.
38. Lü, H.; Gao, J.; Jiang, Z.; Yang, Y.; Song, B.; Li, C., Oxidative desulfurization of dibenzothiophene with molecular oxygen using emulsion catalysis. *Chemical Communications* **2007**, (2), 150-152.
39. Campos-Martin, J. M.; Blanco-Brieva, G.; Fierro, J. L., Hydrogen peroxide synthesis: an outlook beyond the anthraquinone process. *Angewandte Chemie International Edition* **2006**, *45* (42), 6962-6984.
40. Abotsi, G. M.; Scaroni, A. W., A review of carbon-supported hydrodesulfurization catalysts. *Fuel Processing Technology* **1989**, *22* (2), 107-133.
41. Long, R. B.; Caruso, F. A., Selective separation of heavy oil using a mixture of polar and nonpolar solvents. Google Patents: 1985.

42. Zaykina, R.; Zaykin, Y. A.; Mirkin, G.; Nadirov, N., Prospects for irradiation processing in the petroleum industry. *Radiation Physics and Chemistry* **2002**, *63* (3-6), 617-620.
43. Shah, Y. T.; Pandit, A.; Moholkar, V., *Cavitation reaction engineering*. Springer Science & Business Media: 1999.
44. Yen, T.; Gilbert, R.; Fendler, J., Membrane mimetic chemistry and its applications. New York: Plenum Press: 1994.
45. Tu, S. P.; Yen, T. F., The feasibility studies for radical-induced decomposition and demetalation of metalloporphyrins by ultrasonication. *Energy & fuels* **2000**, *14* (6), 1168-1175.
46. Mei, H.; Mei, B.; Yen, T. F., A new method for obtaining ultra-low sulfur diesel fuel via ultrasound assisted oxidative desulfurization. *Fuel* **2003**, *82* (4), 405-414.
47. Liu, W.-Y.; Lei, Z.-L.; Wang, J.-K., Kinetics and mechanism of plasma oxidative desulfurization in liquid phase. *Energy & fuels* **2001**, *15* (1), 38-43.
48. Dehkordi, A. M.; Kiaei, Z.; Sobati, M. A., Oxidative desulfurization of simulated light fuel oil and untreated kerosene. *Fuel Processing Technology* **2009**, *90* (3), 435-445.
49. Yu, G.; Lu, S.; Chen, H.; Zhu, Z., Diesel fuel desulfurization with hydrogen peroxide promoted by formic acid and catalyzed by activated carbon. *Carbon* **2005**, *43* (11), 2285-2294.
50. Farshi, A.; Shiralizadeh, P., Sulfur reduction of heavy fuel oil by oxidative desulfurization (ODS) method. *Petroleum & Coal* **2015**, *57* (3).
51. Hajivand, A.; Mirkamali, A.; Safari, F.; Sarvai Sarmidani, O., Government criminal responsibility for environmental crimes in Iran: Necessities and challenges. *Environmental Sciences* **2018**, *16* (2), 65-82.
52. Ali, M. F.; Al-Malki, A.; El-Ali, B.; Martinie, G.; Siddiqui, M. N., Deep desulphurization of gasoline and diesel fuels using non-hydrogen consuming techniques. *Fuel* **2006**, *85* (10-11), 1354-1363.
53. Jaafar, N. F.; Jalil, A. A.; Triwahyono, S.; Shamsuddin, N., New insights into self-modification of mesoporous titania nanoparticles for enhanced photoactivity: Effect of microwave power density on formation of oxygen vacancies and Ti^{3+} defects. *RSC advances* **2015**, *5* (110), 90991-91000.

54. Shafiq, I.; Shafique, S.; Akhter, P.; Abbas, G.; Qurashi, A.; Hussain, M., Efficient catalyst development for deep aerobic photocatalytic oxidative desulfurization: recent advances, confines, and outlooks. *Catalysis reviews* **2022**, *64* (4), 789-834.
55. Saito, H.; Nosaka, Y., Mechanism of singlet oxygen generation in visible-light-induced photocatalysis of gold-nanoparticle-deposited titanium dioxide. *The Journal of Physical Chemistry C* **2014**, *118* (29), 15656-15663.
56. Wu, D.; Li, J.; Guan, J.; Liu, C.; Zhao, X.; Zhu, Z.; Ma, C.; Huo, P.; Li, C.; Yan, Y., Improved photoelectric performance via fabricated heterojunction g-C₃N₄/TiO₂/HNTs loaded photocatalysts for photodegradation of ciprofloxacin. *Journal of Industrial and Engineering Chemistry* **2018**, *64*, 206-218.
57. Groysman, A., *Corrosion in systems for storage and transportation of petroleum products and biofuels: identification, monitoring and solutions*. Springer Science & Business Media: 2014.
58. Xiong, L.-B.; Li, J.-L.; Yang, B.; Yu, Y., Ti³⁺ in the surface of titanium dioxide: generation, properties and photocatalytic application. *Journal of Nanomaterials* **2012**, *2012*, 9-9.
59. Zhao, C.; Pelaez, M.; Dionysiou, D. D.; Pillai, S. C.; Byrne, J. A.; O'Shea, K. E., UV and visible light activated TiO₂ photocatalysis of 6-hydroxymethyl uracil, a model compound for the potent cyanotoxin cylindrospermopsin. *Catalysis today* **2014**, *224*, 70-76.
60. Kalantari, K.; Kalbasi, M.; Sohrabi, M.; Royaei, S. J., Synthesis and characterization of N-doped TiO₂ nanoparticles and their application in photocatalytic oxidation of dibenzothiophene under visible light. *Ceramics International* **2016**, *42* (13), 14834-14842.
61. Wang, B.; Zhu, J.; Ma, H., Desulfurization from thiophene by SO₄²⁻/ZrO₂ catalytic oxidation at room temperature and atmospheric pressure. *Journal of Hazardous Materials* **2009**, *164* (1), 256-264.
62. Zarrabi, M.; Entezari, M. H.; Goharshadi, E. K., Photocatalytic oxidative desulfurization of dibenzothiophene by C/TiO₂@ MCM-41 nanoparticles under visible light and mild conditions. *RSC Advances* **2015**, *5* (44), 34652-34662.
63. Fox, M. A.; Abdel-Wahab, A., Selectivity in the TiO₂-mediated photocatalytic oxidation of thioethers. *Tetrahedron letters* **1990**, *31* (32), 4533-4536.

64. Jusoh, R.; Jalil, A. A.; Triwahyono, S.; Kamarudin, N., Synthesis of dual type Fe species supported mesostructured silica nanoparticles: synergistical effects in photocatalytic activity. *RSC Advances* **2015**, *5* (13), 9727-9736.
65. Wang, X.-j.; Li, F.-t.; Liu, J.-x.; Kou, C.-g.; Zhao, Y.; Hao, Y.-j.; Zhao, D., Preparation of TiO₂ in ionic liquid via microwave radiation and in situ photocatalytic oxidative desulfurization of diesel oil. *Energy & fuels* **2012**, *26* (11), 6777-6782.
66. Bakar, S. A.; Byzynski, G.; Ribeiro, C., Synergistic effect on the photocatalytic activity of N-doped TiO₂ nanorods synthesised by novel route with exposed (110) facet. *Journal of Alloys and Compounds* **2016**, *666*, 38-49.
67. Li, F.-t.; Liu, Y.; Sun, Z.-m.; Zhao, Y.; Liu, R.-h.; Chen, L.-j.; Zhao, D.-s., Photocatalytic oxidative desulfurization of dibenzothiophene under simulated sunlight irradiation with mixed-phase Fe₂O₃ prepared by solution combustion. *Catalysis Science & Technology* **2012**, *2* (7), 1455-1462.
68. Robertson, J.; Bandosz, T. J., Photooxidation of dibenzothiophene on TiO₂/hectorite thin films layered catalyst. *Journal of Colloid and Interface Science* **2006**, *299* (1), 125-135.
69. Zhang, Y.; Wang, L.; Zhang, N.; Zhou, Z., Adsorptive environmental applications of MXene nanomaterials: a review. *RSC advances* **2018**, *8* (36), 19895-19905.
70. Arora, C.; Soni, S.; Sahu, S.; Mittal, J.; Kumar, P.; Bajpai, P., Iron based metal organic framework for efficient removal of methylene blue dye from industrial waste. *Journal of Molecular Liquids* **2019**, *284*, 343-352.
71. Kuang, Y.; Zhang, X.; Zhou, S., Adsorption of methylene blue in water onto activated carbon by surfactant modification. *Water* **2020**, *12* (2), 587.
72. Nguyen, V.-H.; Nguyen, B.-S.; Hu, C.; Nguyen, C. C.; Nguyen, D. L. T.; Nguyen Dinh, M. T.; Vo, D.-V. N.; Trinh, Q. T.; Shokouhimehr, M.; Hasani, A., Novel architecture titanium carbide (Ti₃C₂T_x) MXene cocatalysts toward photocatalytic hydrogen production: a mini-review. *Nanomaterials* **2020**, *10* (4), 602.
73. Zhang, L.; Chen, D.; Jiao, X., Monoclinic structured BiVO₄ nanosheets: hydrothermal preparation, formation mechanism, and coloristic and

- photocatalytic properties. *The Journal of Physical Chemistry B* **2006**, *110* (6), 2668-2673.
74. Malathi, A.; Madhavan, J.; Ashokkumar, M.; Arunachalam, P., A review on BiVO₄ photocatalyst: activity enhancement methods for solar photocatalytic applications. *Applied Catalysis A: General* **2018**, *555*, 47-74.
75. Hu, Y.; Fan, J.; Pu, C.; Li, H.; Liu, E.; Hu, X., Facile synthesis of double cone-shaped Ag₄V₂O₇/BiVO₄ nanocomposites with enhanced visible light photocatalytic activity for environmental purification. *Journal of Photochemistry and Photobiology A: Chemistry* **2017**, *337*, 172-183.
76. Lv, D.; Zhang, D.; Pu, X.; Kong, D.; Lu, Z.; Shao, X.; Ma, H.; Dou, J., One-pot combustion synthesis of BiVO₄/BiOCl composites with enhanced visible-light photocatalytic properties. *Separation and Purification Technology* **2017**, *174*, 97-103.
77. He, H.; Berglund, S. P.; Rettie, A. J.; Chemelewski, W. D.; Xiao, P.; Zhang, Y.; Mullins, C. B., Synthesis of BiVO₄ nanoflake array films for photoelectrochemical water oxidation. *Journal of Materials Chemistry A* **2014**, *2* (24), 9371-9379.
78. Karunakaran, C.; Kalaivani, S.; Vinayagamoorthy, P.; Dash, S., Electrical, optical and visible light-photocatalytic properties of monoclinic BiVO₄ nanoparticles synthesized hydrothermally at different pH. *Materials Science in Semiconductor Processing* **2014**, *21*, 122-131.
79. Ke, D.; Peng, T.; Ma, L.; Cai, P.; Jiang, P., Photocatalytic water splitting for O₂ production under visible-light irradiation on BiVO₄ nanoparticles in different sacrificial reagent solutions. *Applied Catalysis A: General* **2008**, *350* (1), 111-117.
80. Ren, L.; Jin, L.; Wang, J.-B.; Yang, F.; Qiu, M.-Q.; Yu, Y., Template-free synthesis of BiVO₄ nanostructures: I. Nanotubes with hexagonal cross sections by oriented attachment and their photocatalytic property for water splitting under visible light. *Nanotechnology* **2009**, *20* (11), 115603.
81. Shang, M.; Wang, W.; Zhou, L.; Sun, S.; Yin, W., Nanosized BiVO₄ with high visible-light-induced photocatalytic activity: ultrasonic-assisted synthesis and protective effect of surfactant. *Journal of Hazardous Materials* **2009**, *172* (1), 338-344.

82. Venkatesan, R.; Velumani, S.; Kassiba, A., Mechanochemical synthesis of nanostructured BiVO_4 and investigations of related features. *Materials Chemistry and Physics* **2012**, *135* (2-3), 842-848.
83. García-Pérez, U.; Sepúlveda-Guzmán, S.; Martínez-De La Cruz, A., Nanostructured BiVO_4 photocatalysts synthesized via a polymer-assisted coprecipitation method and their photocatalytic properties under visible-light irradiation. *Solid state sciences* **2012**, *14* (3), 293-298.
84. Wang, M.; Liu, Q.; Luan, H. Y. In *Preparation, characterization and photocatalytic preoperty of BiVO_4 photocatalyst by sol-gel method*, Applied Mechanics and Materials, Trans Tech Publ: 2011; pp 1307-1311.
85. Li, B.; Song, H.; Han, F.; Wei, L., Photocatalytic oxidative desulfurization and denitrogenation for fuels in ambient air over $\text{Ti}_3\text{C}_2/\text{g-C}_3\text{N}_4$ composites under visible light irradiation. *Applied Catalysis B: Environmental* **2020**, *269*, 118845.
86. Hitam, C.; Jalil, A.; Abdurashed, A., A review on recent progression of photocatalytic desulphurization study over decorated photocatalysts. *Journal of Industrial and Engineering Chemistry* **2019**, *74*, 172-186.
87. Imtiaz, F.; Rashid, J.; Xu, M., Semiconductor nanocomposites for visible light photocatalysis of water pollutants. *Concepts of Semiconductor Photocatalysis* **2019**.
88. Sadegh, H.; Shahryari-ghoshekandi, R.; Kazemi, M., Study in synthesis and characterization of carbon nanotubes decorated by magnetic iron oxide nanoparticles. *International Nano Letters* **2014**, *4*, 129-135.
89. Reddy, B., *Advances in nanocomposites: synthesis, characterization and industrial applications*. BoD–Books on Demand: 2011.
90. La Rosa, A.; Yan, M.; Fernandez, R.; Wang, X.; Zegarra, E., Top-down and Bottom-up approaches to nanotechnology.
91. Guglielmi, M.; KICKELBICK, G.; Martucci, A., *Sol-gel nanocomposites*. Springer: 2014.
92. Zhang, H.; Chen, G., Potent antibacterial activities of Ag/TiO_2 nanocomposite powders synthesized by a one-pot sol– gel method. *Environmental Science & Technology* **2009**, *43* (8), 2905-2910.
93. Chen, D.-H.; He, X.-R., Synthesis of nickel ferrite nanoparticles by sol-gel method. *Materials Research Bulletin* **2001**, *36* (7-8), 1369-1377.

94. Murdoch, M.; Waterhouse, G.; Nadeem, M.; Metson, J.; Keane, M.; Howe, R.; Llorca, J.; Idriss, H., The effect of gold loading and particle size on photocatalytic hydrogen production from ethanol over Au/TiO₂ nanoparticles. *Nature Chemistry* **2011**, *3* (6), 489-492.
95. Xu, W.-p.; Zheng, L.; Xin, H.; Lin, C.; Okuyama, M., Formation of BaTiO₃ and PbTiO₃ thin films under mild hydrothermal conditions. *Journal of Materials Research* **1996**, *11* (4), 821-824.
96. Lin, Y.; Lu, C.; Wei, C., Microstructure and photocatalytic performance of BiVO₄ prepared by hydrothermal method. *Journal of Alloys and Compounds* **2019**, *781*, 56-63.
97. Iyyapushpam, S.; Nishanthi, S.; Padiyan, D. P., Photocatalytic degradation of methyl orange using α -Bi₂O₃ prepared without surfactant. *Journal of Alloys and Compounds* **2013**, *563*, 104-107.
98. Mergen, Ö. B.; Arda, E., Determination of optical band gap energies of CS/MWCNT bio-nanocomposites by Tauc and ASF methods. *Synthetic Metals* **2020**, *269*, 116539.
99. Masnadi-Shirazi, M.; Lewis, R.; Bahrami-Yekta, V.; Tiedje, T.; Chicoine, M.; Servati, P., Bandgap and optical absorption edge of GaAs^{1-x}Bi_x alloys with 0 < x < 17.8%. *Journal of Applied Physics* **2014**, *116* (22), 223506.
100. Hameeda, B.; Mushtaq, A.; Saeed, M.; Munir, A.; Jabeen, U.; Waseem, A., Development of Cu-doped NiO nanoscale material as efficient photocatalyst for visible light dye degradation. *Toxin Reviews* **2021**, *40* (4), 1396-1406.
101. Zhang, X.; Ai, Z.; Jia, F.; Zhang, L.; Fan, X.; Zou, Z., Selective synthesis and visible-light photocatalytic activities of BiVO₄ with different crystalline phases. *Materials Chemistry and Physics* **2007**, *103* (1), 162-167.
102. Rezvani, M. A.; Khandan, S.; Sabahi, N.; Saeidian, H., Deep oxidative desulfurization of gas oil based on sandwich-type polysilicotungstate supported β -cyclodextrin composite as an efficient heterogeneous catalyst. *Chinese Journal of Chemical Engineering* **2019**, *27* (10), 2418-2426.
103. Xun, S.; Hou, C.; Li, H.; He, M.; Ma, R.; Zhang, M.; Zhu, W.; Li, H., Synthesis of WO₃/mesoporous ZrO₂ catalyst as a high-efficiency catalyst for catalytic oxidation of dibenzothiophene in diesel. *Journal of Materials Science* **2018**, *53*, 15927-15938.

104. ZHANG, Y.; Lu, W.; ZHANG, Y.; JIANG, Z.; Can, L., Ultra-deep oxidative desulfurization of fuel oil catalyzed by Dawson-type polyoxotungstate emulsion catalysts. *Chinese Journal of Catalysis* **2011**, *32* (1-2), 235-239.
105. Nie, Y.; Dong, Y.; Bai, L.; Dong, H.; Zhang, X., Fast oxidative desulfurization of fuel oil using dialkylpyridinium tetrachloroferrates ionic liquids. *Fuel* **2013**, *103*, 997-1002.
106. Rezvani, M. A.; Shaterian, M.; Akbarzadeh, F.; Khandan, S., Deep oxidative desulfurization of gasoline induced by PMoCu@ MgCu₂O₄-PVA composite as a high-performance heterogeneous nanocatalyst. *Chemical Engineering Journal* **2018**, *333*, 537-544.
107. Pirhashemi, M.; Habibi-Yangjeh, A.; Pouran, S. R., Review on the criteria anticipated for the fabrication of highly efficient ZnO-based visible-light-driven photocatalysts. *Journal of Industrial and Engineering Chemistry* **2018**, *62*, 1-25.
108. Shen, C.; Wang, Y.; Xu, J.; Luo, G., Oxidative desulfurization of DBT with H₂ O₂ catalysed by TiO₂/porous glass. *Green Chemistry* **2016**, *18* (3), 771-781.
109. Lin, F.; Jiang, Z.; Tang, N.; Zhang, C.; Liu, T.; Dong, B., Photocatalytic oxidation of thiophene on RuO₂/SO₄²⁻-TiO₂: Insights for cocatalyst and solid-acid. *Applied Catalysis B: Environmental* **2016**, *188*, 253-258.
110. Zarrabi, M.; Entezari, M. H., Modification of C/TiO₂@ MCM-41 with nickel nanoparticles for photocatalytic desulfurization enhancement of a diesel fuel model under visible light. *Journal of Colloid and Interface Science* **2015**, *457*, 353-359.
111. Hosseini, A.; Faghilian, H., Photocatalytic degradation of benzothiophene by a novel photocatalyst, removal of decomposition fragments by MCM-41 sorbent. *Research on Chemical Intermediates* **2019**, *45* (4), 2383-2401.